International Ocean Discovery Program Expedition 356 Scientific Prospectus

Reefs, Oceans, and Climate

A 5 million year history of the Indonesian Throughflow, Australian monsoon, and subsidence on the northwest shelf of Australia

Stephen J. Gallagher
Co-Chief Scientist
School of Earth Sciences
University of Melbourne
Melbourne VIC 3010
Australia

Craig S. Fulthorpe
Co-Chief Scientist
John A. and Katherine G. Jackson School of Geosciences
University of Texas at Austin
Austin TX 78758-4445
USA

Kara A. Bogus
Expedition Project Manager/Staff Scientist
International Ocean Discovery Program
Texas A&M University
1000 Discovery Drive
College Station TX 77845
USA

Published by
International Ocean Discovery Program

Publisher's notes

This publication was prepared by the International Ocean Discovery Program U.S. Implementing Organization (IODP-USIO): Consortium for Ocean Leadership, Lamont-Doherty Earth Observatory of Columbia University, and Texas A&M University, as an account of work performed under the International Ocean Discovery Program. Funding for the program is provided by the following agencies:

National Science Foundation (NSF), United States

Ministry of Education, Culture, Sports, Science and Technology (MEXT), Japan

European Consortium for Ocean Research Drilling (ECORD)

Ministry of Science and Technology (MOST), People's Republic of China

Korea Institute of Geoscience and Mineral Resources (KIGAM)

Australian Research Council (ARC) and GNS Science (New Zealand), Australian/New Zealand Consortium

Ministry of Earth Sciences (MoES), India

Coordination for Improvement of Higher Education Personnel, Brazil

Disclaimer

This IODP *Scientific Prospectus* is based on precruise Science Advisory Structure panel discussions and scientific input from the designated Co-Chief Scientists on behalf of the drilling proponents. During the course of the cruise, actual site operations may indicate to the Co-Chief Scientists, the Staff Scientist/Expedition Project Manager, and the Operations Superintendent that it would be scientifically or operationally advantageous to amend the plan detailed in this prospectus. It should be understood that any proposed changes to the science deliverables outlined in the plan presented here are contingent upon the approval of the IODP JR Science Operator Director.

Copyright

Citation:
Gallagher, S.J., Fulthorpe, C.S., and Bogus, K.A., 2014. Reefs, oceans, and climate: a 5 million year history of the Indonesian Throughflow, Australian monsoon, and subsidence on the northwest shelf of Australia. *International Ocean Discovery Program Scientific Prospectus,* 356. http://dx.doi.org/10.14379/iodp.sp.356.2014

August 2014

Abstract

The Indonesian Throughflow (ITF) is a critical part of the global thermohaline conveyor. It plays a key role in transporting heat from the equatorial Pacific (the Indo-Pacific Warm Pool) to the Indian Ocean and exerts a major control on global climate. The complex tectonic history of the Indonesian Archipelago, a result of continued northward motion and impingement of the Australasian Plate into the Southeast Asian part of the Eurasian Plate, makes it difficult to reconstruct long-term (i.e., million year) ITF history from sites within the archipelago. The best areas to investigate ITF history are downstream in the Indian Ocean, either in the deep ocean away from strong tectonic deformation or along proximal passive margins that are directly under the influence of the ITF. Although previous Ocean Drilling Program and Deep Sea Drilling Project deepwater cores recovered in the Indian Ocean have been used to chart Indo-Pacific Warm Pool influence and, by proxy, ITF variability, these sections lack direct biogeographic and sedimentological evidence of the ITF. International Ocean Discovery Program Expedition 356 will drill a transect of cores over 10° latitude on the northwest shelf (NWS) of Australia to obtain a 5 m.y. record of ITF, Indo-Pacific Warm Pool, and climate evolution that has the potential to match orbital-scale deep-sea records in its resolution. Coring the NWS will reveal a detailed shallow-water history of ITF variability and its relationship to climate. It will allow us to understand the history of the Australian monsoon and its variability, a system whose genesis is thought to be related to the initiation of the East Asian monsoon and is hypothesized to have been in place since the Pliocene or earlier. It also will lead to a better understanding of the nature and timing of the development of aridity on the Australian continent.

Detailed paleobathymetric and stratigraphic data from the transect will also allow subsidence curves to be constructed to constrain the spatial and temporal patterns of vertical motions caused by the interaction between plate motion and convection within the Earth's mantle, known as dynamic topography. The NWS is an ideal location to study this phenomenon because it is positioned on the fastest moving continent since the Eocene, on the edge of the degree two geoid anomaly. Accurate subsidence analyses over 10° of latitude can resolve whether northern Australia is moving with/over a time-transient or long-term stationary downwelling within the mantle, thereby vastly improving our understanding of deep-Earth dynamics and their impact on surficial processes.

Schedule for Expedition 356

International Ocean Discovery Program (IODP) Expedition 356 is based on drilling proposal Number 807 FULL (available at **iodp.tamu.edu/scienceops/expeditions/indonesian_throughflow.html**). Following ranking by the IODP Scientific Advisory Structure, the expedition was scheduled for the R/V *JOIDES Resolution*. At the time of publication of this *Scientific Prospectus*, the expedition is scheduled to start in Fremantle, Australia on 31 July 2015 and end in Darwin, Australia on 30 September 2015. A total of 56 days will be available for the transit, drilling, coring, and downhole measurements described in this report (for the current detailed schedule, see **iodp.tamu.edu/scienceops/**). Further details about the facilities aboard the *JOIDES Resolution* can be found at **iodp.tamu.edu/labs/ship.html.**

Introduction

During the past 5 m.y., Earth's climate has experienced a major transition from the mid-Pliocene warmth to the Late Pleistocene ice ages (Rohling et al., 2014). Although we now have increasing numbers of high-resolution records of climate variability from ocean basins in both high-latitude and equatorial regions (McClymont et al., 2013), high-resolution information for the northwestern region of Australia and from other shelfal areas worldwide is rare. The wedge of sediment that has accumulated over the last 5 m.y. on the northwest shelf (NWS) of Australia epitomizes the geological history of Australia's northern margin (Fig. **F1**). The section is made up of a variety of sediment types including subtropical to tropical shelf calcarenite, calcilutite, marl, and deepwater mudstone and siltstone eroded by submarine canyons (Wallace et al., 2003). In combination, these sediments make up a prograding shelf-type system typical of much of the Australian continental margin (Wallace et al., 2002).

The foci of Expedition 356 fall under three main headings.

Indonesian Throughflow, Leeuwin Current, and reef development

During the late Neogene, the NWS has acted as a subsiding platform upon which most contemporary environmental changes are recorded. Located at the fringes of the Indo-Pacific Warm Pool, this margin is therefore an ideal region in which to study tropical oceanography (Rosleff-Soerensen et al., 2012) and the history of the Indonesian Throughflow (ITF). The ITF also helps drive the Leeuwin Current, which is the

only southward flowing eastern boundary current in the Southern Hemisphere (Cresswell, 1991; Pearce, 2009). This current extended tropical reef development to 29°S during the Late Pleistocene (Collins et al., 2006). The orbital-scale variability of the Leeuwin Current can be estimated using tropical sedimentary (coral reefs and ooids) and fossil biogeographic indexes, so we can determine by proxy the underlying controls that triggered Pliocene–Pleistocene reef development. Coring a latitudinal transect from 18°S to 27°S will provide essential information as to whether the switch to tropical sedimentation was synchronous or diachronous in this region as well as a long-term perspective on how coral reefs in the east Indian Ocean developed through variable climatic conditions.

Australian monsoon and continental aridity

The continental shelf in this region lies directly offshore the semi-arid Australian continent climatically dominated by the Australian monsoon (Suppiah, 1992). Shelf/slope sediments therefore host a vast but barely explored archive of late Neogene climate variability (van der Kaars and De Deckker, 2002). Recovering cores from the NWS will increase our understanding of the long-term geographic controls on Australian monsoonal variability and its relationship to the onset of aridity in Australia (McLaren et al., 2014).

Subsidence and geodynamics of Australian plate

Obtaining high-resolution stratigraphic data from the NWS will lead to improved burial and subsidence estimates for this region. These data will enable us to decipher the contribution of large-scale geodynamic processes, such as dynamic topography, on the vertical motions of the Earth's surface and associated effects on the NWS sedimentary system (Czarnota et al., 2013).

Background

Tectonic setting

The NWS is a rifted margin that has existed since late Paleozoic time, when Australia was part of eastern Gondwana (Etheridge and O'Brien 1994; Exon and Colwell, 1994; Longley et al., 2002). Ribbon-like microcontinents separated from this part of the

margin in multiple rifting events, with the latest phase of rifting occurring in the Late Jurassic (Heine and Müller, 2005; Exon and Colwell, 1994; Metcalfe, 1988).

Two of our primary sites (NWS-5A and NWS-6A) are in the northern part of the Perth Basin (Fig. **F1**). The remaining sites lie in the Northern Carnarvon Basin (NCB) and Roebuck Basin with an 8 km minimum stratigraphic thickness (Longley et al., 2002; Goncharov, 2004). Here, the earliest rifting occurred during the late Permian (initial breakup of eastern Gondwana; Sengor, 1987). Subsequent rifting episodes occurred during the Late Triassic–Early Jurassic and Late Jurassic (von Rad, Haq, et al., 1992; Driscoll and Karner, 1998) with the final rifting in the latest Jurassic also culminating in earliest Cretaceous separation of greater India from Australia (Boote and Kirk, 1989; von Rad, Haq, et al., 1992; Heine and Müller, 2005). The post-rift thermal subsidence history of the margin has been affected by mild shortening, generally attributed to plate boundary forces resulting from plate reorganization (Romine et al., 1997; Driscoll and Karner, 1998; Sayers et al., 2001; Cathro et al., 2003; Dyksterhuis et al., 2005). The most recent major nearby tectonic event was the late Miocene collision between northern Australia and the Banda arc (Audley-Charles et al., 1988; Lee and Lawver, 1995; Richardson and Blundell, 1996). Although occurring several hundred kilometers to the north of the drilling area, intraplate stresses associated with this ongoing collision have resulted in localized reactivation and inversion of extensional faults in the NCB (Malcolm et al., 1991; Struckmeyer et al., 1998; Cathro et al., 2003).

Oceanographic setting

The Indo-Pacific Warm Pool is a region of warm surface waters (average temperature = 28°C) that covers most of the tropical western Pacific and eastern Indian Oceans (Fig. **F2**). The Indo-Pacific Warm Pool plays a major role in heat transport from low to high latitudes and is subject to decadal scale variability due to the El Niño Southern Oscillation (de Garidel-Thoron et al., 2005). The intensity of the Indo-Pacific Warm Pool functions as a switch in the climate system, and it is consequently a key influence on long- and short-term global climate change (Xu et al., 2006). Therefore, the history of the Indo-Pacific Warm Pool is crucial to our understanding of the global climatic and oceanic systems, as well as their regional effects on the NWS.

Climatic cooling since 15 Ma and an evolving tectonic configuration created appropriate boundary conditions to generate “near-modern” oceanic conditions in the Indo-Pacific. The Indo-Pacific Warm Pool (Fig. **F2**) is trapped by the Indonesian archipelago and released into the Indian Ocean via the ITF (Gordon, 2005). The ITF trans-

ports 10–15 Sverdrups (1 Sv = 10^6 m^3/s) of low-salinity warm water via the Indonesian archipelago (Kuhnt et al., 2004) to the Indian Ocean, forming an important switching point in the global thermohaline conveyor.

The extratropical shelf regions of the Indo-Pacific are strongly influenced by shallow (50–300 m) currents that originate in the Indo-Pacific Warm Pool region. For example, the NWS oceanography from 5° to 15°S is dominated by the South Equatorial Current (Collins, 2002; Fig. **F2**). South of 15°S, the shallow and narrow Leeuwin Current (Fig. **F2**) (<100 km wide, <300 m deep) transports warm, low-salinity nutrient-deficient water southward along the west coast of Australia (Pattiaratchi, 2006). It is driven by long-shore winds and an upper-ocean pressure gradient (upper 250–300 m) (Tomczak and Godfrey, 1994) that overcomes equator-ward wind stress and upwelling to flow south (Pattiaratchi, 2006). Another driver for this current is the steric height difference between the low density and salinity Timor Sea and the cooler, denser, saline waters off the coast of Perth. It is the only south-flowing eastern boundary current in the Southern Hemisphere and has an enormous effect on the climate of the region. The Leeuwin Current extends modern coral reef development to 29°S (the Houtman-Abrolhos reefs, Fig. **F1**) (Collins et al., 1993) and the tropical–subtropical transition as far south as Rottnest Island (33°S; Greenstein and Pandolfi, 2008). Although the Late Pleistocene record and modern oceanography of the Leeuwin Current are well understood (see Cresswell, 1991; Pearce, 2009, and references therein), the pre-Late Pleistocene history of this current is not well known (Kendrick et al., 1991; Wyroll et al., 2009). James et al. (1999) suggested that the Leeuwin Current ceased during glacial periods and restarted during interglacials. Kendrick et al. (1991) used fossil mollusks to suggest that onset of the Leeuwin Current occurred <500 ka, whereas Sinha et al. (2006) and Karas et al. (2011) suggested onset at 2.5 Ma, and McGowran et al. (1997) proposed a Late Eocene (40 Ma) onset age. However, Gallagher et al. (2009; in press) used subsurface well cutting data from the NWS to suggest that the "modern" Leeuwin Current is younger than 1 Ma.

Climate and paleoclimate setting

The arid to semiarid conditions of the Australian interior extend to the west coast of Australia. In the north, rainfall is erratic but predominantly monsoonal (Fig. **F2**) with the summer rainfall dominance declining sharply toward the south (Sturman and Tapper, 2005). Warm, moist, equatorial air is the major source of monsoonal and cyclonic rain in the north but is replaced in the south by tropical air from the Indian Ocean, which is also known as the "pseudomonsoon" (Gentilli, 1972). The marine

pollen record from 6-1.8 Ma at Ocean Drilling Program (ODP) Site 765 (15°S; Fig. **F1**) shows progressive aridity through the replacement of sclerophyll forest (dominated by Casuarinaceae and grassland) with increased saltbush from 5-3 Ma, and particularly since 1.8 Ma (McMinn and Martin, 1992; Martin and McMinn, 1994). By contrast, <1 Ma strata yield sufficient *Eucalyptus* species to indicate woodland cover, but it is not clear whether this is related to increased rainfall or an evolutionary change associated with higher burning levels. A marine core (GC17) (Fig. **F1**) from offshore Cape Range shows marked changes in total and seasonal rainfall in the last 100 k.y. with changing monsoon intensity (van der Kaars and De Deckker, 2002). Climate variation has been quantified for this record using transfer functions from core-top pollen samples in the region (van der Kaars et al., 2006).

Sedimentation history

The northward drift of Australia led to a transition from siliciclastic to predominantly carbonate deposition on the NWS. Carbonate sedimentation was already dominant by the Eocene, although a siliciclastic component persisted (Hull and Griffiths, 2002). This drift brought the NWS into tropical latitudes (Veevers et al., 1991; Müller et al., 2008a); the region had reached 36°–40°S by the early Oligocene and is now at 18°–22°S. Prograding carbonate clinoforms developed in the early Oligocene and continued to the Miocene (Hull and Griffiths, 2002; Cathro et al., 2003). Late early Oligocene–early late Miocene carbonate sediments are heterozoan (i.e., derived from light-independent organisms) and include benthic foraminifers with subordinate bryozoa and rare coral fragments (Cathro et al., 2003). Such sediments develop unrimmed platforms lacking reefs. Resulting clinoformal sequences comprise fine-grained calcilutites on the slope, a mixture of calcisiltites and calcarenites near clinoform rollovers (equivalent to paleoshelf edges), and calcarenites on paleoshelves (Hull and Griffiths, 2002; Moss et al., 2004). Evidence for pre-Quaternary reef development is limited; seismically identified reefs or reef mounds occur in the Oligocene–Miocene section (Romine et al., 1997; Cathro et al., 2003; Ryan et al., 2009; Liu et al., 2011). Rare reefs also occur in the Pliocene–Quaternary section (Ryan et al., 2009), and conditions were favorable for late Quaternary reef development even farther south to 28°S (Collins, 2002). However, sedimentation rates, even in temperate water carbonates, can be high (>40 cm/k.y.), comparable to the lower end of the spectrum of tropical carbonate platform growth rates (James and Bone, 1991).

Previous drilling in the region

The NWS has been extensively drilled by industry over the last 40 y (Longley et al., 2002). As a result, well (cuttings) and existing seismic data assisted with our site choices. However, cores that sample the upper kilometer (Miocene to Holocene carbonate section) are extremely rare. The only continuous cores that exist are from engineering boreholes, typically sampling Late Pleistocene carbonates in the upper 100 m (Fig. **F3**), and intermittent sidewall cores (Fig. **F4**). Expedition 356 primary sites redrill six pre-existing industry wells (Table **T1**) where hydrocarbons are known to be absent from the targeted section. Alternate sites are also located near the primary sites (Fig. **F1**). All supporting site data for Expedition 356 are archived at the **IODP Site Survey Data Bank.**

The sites lie along a latitudinal transect designed to sample the lateral variability in subsidence and tropical conditions along the NWS over the last 5 m.y. (Fig. **F1**). The wells adjacent to the primary sites have gamma wireline logs (mostly to the seabed) (Fig. **F5**) and cutting samples. Additionally, there are two continuously cored engineering bores (BHC4 and BHC1) near the Angel-1 well (19.5°S; Figs. **F1, F3**). Facies data (%$CaCO_3$) from these are directly comparable to the LR2004 oxygen isotope record (Lisiecki and Raymo, 2005). For example, the lower carbonate marly facies (with relatively high gamma response) were deposited during interglacial highstands, and the high-carbonate calcarenites (with ooids) were deposited as the sea level fell during glacials. It is likely the presence of increased siliciclastics (gamma peaks) on the NWS is related to increased precipitation and terrestrial runoff across the shelf during the interglacial periods from an enhanced Australian monsoon. The decrease in terrestrial input during glacials was due to increasingly arid conditions, starving the shelf of siliciclastics (Gallagher et al., in press). This sedimentation model is likely applicable throughout the Pliocene–Pleistocene shelfal carbonate section (Figs. **F5, F6**) because regional subsidence has likely facilitated the preservation of the majority of the eccentricity/obliquity-controlled eustatic cycles throughout this period (Fig. **F6**).

In addition, the gamma log pattern clearly changes through time: Pliocene strata are more gamma-rich and there is a secular shift to lower values during the Pleistocene (Figs. **F5, F6**). This could reflect progressive changes in shelf geometry; however, this effect can be "filtered" out using paleobathymetric estimates in each section. Furthermore, the prevalence of this upward decreasing gamma pattern across 10° of latitude suggests a more regional mechanism, such as an increase of aridity through time and decreasing influence of the Australian monsoon.

The shelfal sections also yield well-preserved *Globigerinoides ruber* and *Cibicidoides* spp. (plus many other benthic foraminiferal species) in the interglacial marly facies. The *G. ruber* and *Cibicidoides* spp. exhibit isotope values close to deep-sea Pleistocene values in the region (Wells and Wells, 1994), providing an opportunity to use proxy data for salinity and temperature variations (such as paired Mg/Ca and $\delta^{18}O$ analyses) for each glacial cycle to investigate the shallow-water (<200 m) influence of the Indo-Pacific Warm Pool and ITF on the region and their relationship to the Leeuwin Current.

Chronostratigraphic framework

A robust chronostratigraphic framework is particularly important for this expedition. This should be possible for each site, and a wealth of information is already available.

Biostratigraphy

Planktonic foraminifers and nannofossils are common in NWS shelfal sections, especially the highstand and outer-shelf to upper-slope facies, but they are absent in the oolitic facies and poorly preserved in the coarse calcarenites. They are abundant in all the facies of the West Tryal Rocks-1 well (near Site NWS-4A; see data and zonation in Gallagher et al., 2009). There are also a few useful dinoflagellate datums (McMinn, 1992, 2002) in the Pliocene–Pleistocene section to assist age calibration.

Magnetostratigraphy

Typically, this technique is used to provide a chronostratigraphy for deepwater siliciclastics or carbonates. However, Sakai and Jige (2006) successfully demonstrated that it can also be useful in calibrating Pleistocene shallow-water tropical carbonates in the Ryukyus (Japan), so that it should work well in the finer grained, more marly facies of the NWS.

Correlation to oxygen isotope curves

With a few biostratigraphic calibration points, it is possible to correlate log gamma maxima to interglacial cycles (Gallagher et al., in press), similar to the approach adopted by Carter and Gammon (2004). These authors correlated the gamma profile from ODP Site 1119 to oxygen isotope data to achieve a millennial-scale record of New Zealand upper slope sedimentation for the last 3.9 m.y. This type of wireline analysis has also revealed Pliocene–Pleistocene 40 k.y. scale climate variability in the Japan Sea (deMenocal et al., 1992).

Carbon isotope dating

There are sufficiently well preserved mollusks in the upper parts of the sections to permit carbon isotope dating. This technique has already been applied successfully near the top of Core BHC4 (Fig. **F3**).

Strontium isotope dating

With thorough petrographic screening for diagenetic effects, such as subaerial exposure, it is possible to use strontium isotopes from bioclasts to construct age-depth profiles. Ehrenberg et al. (2006) have successfully dated calcitic bioclasts, such as bivalves, red algae, and large benthic foraminifers, from Miocene platform carbonates. It is likely that we will encounter such macrofossils in most of the shelfal sequences.

Scientific objectives

The interpretation of past climate records to inform our future is one of the major themes of the IODP Science Plan (2013–2023). Expedition 356 will focus on the 5 m.y. marine history of a rifted margin downstream of a major arm of the global thermohaline conveyor (transported via the ITF) to understand the onset and variability of key oceanographic and climate features. We are particularly interested in the relationship between ocean gateways and marine conditions in the transition from the warmer early Pliocene to the cooler Pleistocene and in factors controlling the onset and variability of the Australian monsoon. Results from this expedition will also reveal insights into gateway tectonic history, paleobathymetry, and subsidence.

We will drill, core, and log a latitudinal transect from 18°S to 28°S (Fig. **F1**) to achieve three key objectives:

1. Determine the timing and variability of the ITF, Indo-Pacific Warm Pool, and onset of the Leeuwin Current to understand the controls on Quaternary extra-tropical carbonate and reef deposition.
2. Obtain an ~5 m.y. orbital-scale tropical to subtropical climate and ocean archive, directly comparable to deep-ocean oxygen isotope and ice-core archives, to chart the variability of the Australian monsoon and the onset of aridity in northwestern Australia.
3. Provide empirical input into the spatio-temporal patterns of subsidence along the NWS that can be used to place fundamental constraints on the interaction

between Australian plate motion and mantle convection and to groundtruth geodynamic models.

1. Determine the timing and variability of the ITF, Indo-Pacific Warm Pool, and onset of the Leeuwin Current to understand the controls on extra-tropical carbonate and reef deposition.

The ITF cannot be considered in terms of an "open" or "closed" gateway but instead as the interaction between (1) the source of the water (south versus north Pacific), (2) the location of the main outlet, and (3) variable sill depths and locations through time (Kuhnt et al., 2004). The current eastern (main) outlet through the Timor Sea probably originated around 2–2.5 Ma. Until then, the Bali-Lombok Strait was more important (Kuhnt et al., 2004; Hall, 2009). We intend to document ITF influence on the NWS using fossil biogeography/geochemistry and sedimentary/seismic facies.

Fossil biogeography and geochemistry

The early history of the Indo-Pacific Warm Pool in the Indo-Pacific region has been interpreted from planktonic microfossils. Kennett et al. (1985) suggested that the Indo-Pacific Warm Pool formed as a result of Indonesian seaway closure at ~8 Ma. In contrast, Srinivasan and Sinha (1998) used planktonic foraminiferal biogeography to suggest its formation at ~5.2 Ma. Jian et al. (2006) suggested a late Miocene (~10 Ma) Indo-Pacific Warm Pool with the "modern" warm pool developing at ~4 Ma. Karas et al. (2011) used comparisons between the Mg/Ca and stable isotope data from ODP Holes 709C and 763A on the western and eastern sides of the Indian Ocean, respectively (Fig. **F1**), to suggest ITF restriction from 3.5-3 Ma that caused 3°C cooling in the region (Fig. **F4**). Preliminary biogeographic analyses of NWS well cuttings by Gallagher et al. (2009) showed that particular shelfal benthic foraminifers species (*Asterorotalia* spp., *Pseudorotalia* spp., and *Heterolepa margaritiferus*) migrate to the NWS from the southwest Pacific with the waxing and waning of the ITF. Elsewhere, these taxa have proven useful tracers of the warmer Tsushima Current offshoot of the Kuroshio Current in the Japan Sea (Hoiles et al., 2012). Further foraminiferal analyses of 60 sidewall cores from the Fisher-1 well (near primary Site NWS-3A) reveal at least three periods of ITF restriction during the Pliocene (Fig. **F4**). Gallagher et al. (2009) also used these species to interpret the onset of a relatively more intense Leeuwin Current and ITF ~1 Ma during the Middle Pleistocene transition.

Palynomorphs are also useful tracers of Leeuwin Current flow. For example, pteridophyta spores with Indonesian affinities have been found in surface (modern) and sub-

surface Late Pleistocene marine sediment on the NWS (van der Kaars and De Deckker, 2002, 2003). Spooner et al. (2011) documented 500 k.y. of Leeuwin Current variability from a deep-sea core (MD002361, 1805 m water depth) (Fig. **F1**) using stable isotopes and planktonic foraminiferal proxies and suggested a weaker Leeuwin Current during glacial periods, when the West Australian Current was dominant, and a stronger Leeuwin Current during interglacials, especially marine isotope stage (MIS) 11. The southerly migration of Indo-Pacific mollusks and corals to southwest Australia has also been used to document the Late Pleistocene history of the Leeuwin Current (Kendrick et al., 1991; Greenstein and Pandolfi, 2008). Therefore, a combination of benthic foraminiferal, palynological, and macrofossil analyses will be helpful to chart ITF onset and variability and to trace Leeuwin Current activity through time. Further insights into this variability can be achieved using paired C/O isotope and Mg/Ca analyses of foraminifers from NWS glacial–interglacial cycles to interpret middle to outer shelf temperature variations that might reflect the waxing and waning of the ITF. These data will strongly complement nearby Pliocene–Pleistocene deep-sea records (Karas et al. 2009, 2011; Spooner et al. 2011; Stuut et al., 2014).

Transition to warm-water carbonate development

Warm-water carbonates are dominated by photozoan organisms (i.e., organisms relying on photosymbionts, such as corals). Two key features that distinguish tropical from non-tropical carbonates are the presence of coral reefs and ooids (Clarke, 2009; Bosence, 2009). Coral reefs are confined to seawater >18°C (Kleypas et al., 1999). Ooids form at temperatures >20°C with salinities >37‰ (Lees and Buller, 1972). We hypothesize that these two key diagnostic tropical features appear late in the history of the NWS, first developing during the Pleistocene south of 18°S, and that they become progressively younger southward.

Determining the timing and history of late Neogene reef development

The distribution and timing of coral reef development in west Australia is intimately related to the Leeuwin Current (Kendrick et al., 1991). Collins (2002) summarized late Neogene reef distribution in northwest Australia by describing a series of late Tertiary reefs that have developed discontinuously over time. The late Quaternary stratigraphic evolution of Scott (14°S), Rowley Shoals (17.3°S), Ningaloo (22.7°S), and Houtman-Abrolhos (28°S) reefs (Fig. **F1**) is related to a combination of increased subsidence amplitude toward the north, variability in the Leeuwin Current, and sea level change (Collins and Testa, 2010). Earlier reef development is less well constrained. Ryan et al. (2009) described a series of structurally controlled Miocene reefs from 15°S

to 18°S (Fig. F1) using seismic data. These interpreted reefs drowned at the end of the late Miocene (Messinian) when they failed to keep up with sea level change. Further south (22°S), Cathro et al. (2003) interpreted possible Miocene "barrier" reefs or mounds in seismic data. Liu et al. (2011) also interpreted possible Miocene reefs based on seismically imaged mounds. Ryan et al. (2009) acknowledged the dearth of post-Miocene and pre-late Quaternary reefs in the region. However, Jones (1973) and Ryan et al. (2009) described an unnamed post-Miocene drowned "fossil" reef imaged using shallow- and deep-penetration seismic data close to the Rowley Shoals (Fig. F1). Another series of drowned fossil reefs are shown in seismic data from 20°S to 22°S (Figs. F1, F7, AF8, AF9).

We hope to date late Neogene reef re-initiation by sampling the platform/slope facies downdip or along strike from fossil reefs imaged by seismic data. For example, Sites NWS-1A and NWS-7A are updip from the buried fossil reef described by Ryan et al. (2009), and parallel, laterally-persistent reflectors connect these locations (Fig. AF15). Therefore, improved ages for these reflectors should allow us to date this reef. In addition, Site NWS-4A is downdip from a drowned reef (Fig. F7), so new age data should similarly constrain its onset (Gallagher et al., in press). Furthermore, downslope transported reefal detritus will enable analyses of reef development in response to variable sea level. Likewise, Site NWS-3A is along strike from several drowned reefs, and data from this site may constrain the ages of their formation. Farther south, Site NWS-6A is directly seaward of and downdip from the Houtman-Abrolhos main reef complex. Dating, coupled with seismic correlation to this complex, will provide insight into its pre-late Quaternary history.

The significance, timing, and onset of ooid formation

Warm waters supersaturated with respect to carbonate are required for marine ooid formation. Ooids are spherical to oval coated grains that typically form in shallow (<5 m), agitated, tide-dominated tropical environments with elevated evaporation and salinity (Simone, 1981; James et al., 2004). Globally, marine subtropical to tropical ooids have been interpreted to be direct evidence of physiochemical precipitation from seawater during periods of elevated alkalinity and supersaturation (Simone, 1981; Rankey and Reeder, 2009). As such, their occurrence in the NWS subsurface may be used as a sea surface temperature, paleobathymetry, and aridity index. Rankey and Reeder (2009) acknowledge the rarity of ooids in modern and pre-Holocene deposits in the Pacific region and suggest that this is due to the relative lack of regions with sufficiently elevated carbonate supersaturation. There is a similar dearth of ooids

in the Indian Ocean (Braithwaite, 1994) for enigmatic reasons. One factor that may account for their rarity in the Indo-Pacific is the absence of particularly favorable conditions required for their formation. For example, ooids accumulate during relatively slow transgressions on flat carbonate platforms (Hearty et al., 2010). If the sea level rise is too fast on a flat platform, they will not form (Hearty et al., 2010). The oldest ooids previously described from the Indian Ocean formed 15.4–12 ka (James et al., 2004) on a low-angle ramp on the NWS (17°S–21°S). James et al. (2004) attributed their formation to increased Leeuwin Current activity (~12 ka) as sea level rose after the Last Glacial Maximum (LGM). Ooids are present in the carbonate supersaturated shallow water of the arid environment in Shark Bay (25.5°S) (Davies, 1970). Other ooids on the NWS (18.5°S) formed 3.3 ka during a period of slow sea level rise (Hearty et al., 2006). In the Maldives, ooids formed during the early cooling and late warming phase of the last glacial cycle (Braithwaite, 1994). Recent work (Gallagher et al., in press) showed that ooids are present in a core dated at 200 ka (Fig. **F3**) and in cuttings younger than 600 ka from the Maitland North-1 well (Fig. **F6**) near primary Site NWS-3A. These represent the oldest recovered ooids in the Indian Ocean, but numerous questions remain. For example:

- When did ooids first occur?
- Does the advent of ooid formation signify the onset of stronger aridity during the last 600 k.y.?
- Is there a paleoceanographic trigger (the ITF?) for ooid formation that resulted in increased alkalinity in the Indian Ocean?
- Is there a relationship between these physiochemical conditions and the onset of reef deposition?
- What is the relationship between glacio-eustatic cycles, aridity, and ooid formation?

We expect to recover shallow-water facies suitable for ooid preservation in the Quaternary intervals at primary Sites NWS-1A/1B, NWS-2A, and NWS-3A and possibly at Sites NWS-5A and NWS-6A.

2. Obtain an ~5 m.y. orbital-scale tropical to subtropical climate and ocean archive, directly comparable to deep-ocean oxygen isotope and ice-core archives, to chart the variability of the Australian monsoon and the onset of aridity in northwestern Australia.

The aridity of Australia is alleviated by the Australian summer monsoon, which delivers substantial precipitation to the northern part of the continent (north of 25°S)

from December to March (Suppiah, 1992; Herold et al., 2011). The winds blow predominantly from the northwest in the rainy season (austral summer), whereas in the dry season (austral winter) the winds blow from the southeast. These changes are associated with the seasonal migration of the subtropical high-pressure belt from 40°S to 30°S. In the austral winter, the Intertropical Convergence Zone (ITCZ) is north of Indonesia and moves south in austral summer to a position immediately north of Australia (Fig. **F2**). The ITCZ moves even farther south over tropical Australia in February and is associated with the peak of the northern Australian wet season (Williams et al., 2009). The Australian monsoon is thought to be caused by land-ocean temperature contrasts and inter-hemispheric flow from the Asian monsoon. Australian monsoon strength and timing is influenced by changes in insolation resulting from obliquity and precessional forcing (Wyrwoll et al., 2007; 2012). The Australian summer monsoon lacks the topographic influence that controls the Indian–East Asian summer monsoon and is therefore weaker and more sensitive to variations in insolation (Wyrwoll et al., 2007). The region affected by the Asian and Australian monsoon systems (70°E to 150°E) is one of the most significant heat sources driving global climate.

The paleomonsoon

An (2000) speculated that the histories of the East Asian and Australian monsoons are linked and that they originated before 7 Ma. Bowman et al. (2010) suggested (in the absence of any definitive northern Australia pre-Quaternary records) that "the (Australian) monsoon is of great antiquity" because of the pronounced diversity and strong adaptations of biota to the wet-dry tropical climate as well as their strong general adaptability. Herold et al. (2011) noted the incomplete knowledge of the nature and intensity of the pre-Quaternary Australian monsoon and investigated its potential impact on rainfall levels in the Miocene using a general circulation model constrained with a vegetation model. Herold et al. (2011) and Greenwood et al. (2012) compiled available paleontological proxy data for the Miocene and reconstructed a seasonally wet northern and interior Australia, supporting a biome (i.e., seasonally dry deciduous vine forests and sclerophyllous woodlands) consistent with a monsoonal precipitation regime wetter than today. The only pollen record from the semiarid northwest Australian continent is west of the Cape Range Peninsula (Core GC17) (Fig. **F1**) and spans the last 100 k.y. (van der Kaars and De Deckker, 2002; van der Kaars et al., 2006). This location is at the southern extremity of the Australian summer monsoon and receives 200–300 mm of rainfall per year, making it ideal to record changes in the latitudinal position of the monsoon (Fig. **F2**). van der Kaars et al.

(2006) used transfer functions to interpret rainfall from the pollen record and hypothesized that a marked reduction in summer rainfall occurred in the absence of monsoonal activity during the LGM. Other deepwater Quaternary records of the Australian monsoon have been obtained from farther north in the Timor Sea (13°S) (Holbourn et al., 2005) and in the Banda Sea (5°S, Beaufort et al., 2010; 8.5°S, Spooner et al., 2005). Holbourn et al. (2005) used foraminiferal and geochemical proxies to chart Timor Sea paleoproductivity over the last 350 k.y. and noted that the Timor Sea productivity record matches the 25°S summer insolation curve, which they interpreted to have strong precessional and eccentricity control. This observation indicates that tropical and/or Southern Hemisphere insolation forcing is an important modulating factor for Australian monsoon intensity. Spooner et al. (2005) combined stable isotope analyses with planktonic foraminiferal assemblages to interpret the 80 k.y. variability of the monsoon and concluded that it was less intense during the first 60 k.y., then intensified at ~15 ka. Beaufort et al. (2010) used calcareous nannofossils to suggest precessional control on primary productivity and Australian monsoon intensity over the last 150 k.y. The Australian monsoon is also interpreted to be broadly controlled by global glacial–interglacial variations (Wyrwoll and Miller, 2001). Strong variations in Australian monsoonal strength between glacial and interglacial periods (paced by orbital eccentricity and precession) have been documented over the last 460 k.y. off northwest Australia (Kawamura et al., 2006) with stronger monsoonal (wet) conditions prevailing during interglacial periods and a weakened monsoon (dry) during glacials. This pattern of glacial–interglacial precipitation variance was further suggested in a 550 k.y. dust record from offshore North West Cape (Stuut et al., 2014). Significant fluvial runoff and megalake expansion across northern and central Australia (Hesse et al., 2004) occurred during interglacials over the last 300 k.y. because of Australian monsoon enhancement. Conversely, reduced precipitation on the NWS (at 23°S) (van der Kaars et al., 2006) and megalake contraction typified glacial conditions (Magee et al., 2004), associated with decreased monsoonal activity.

Charting the 5 m.y. record of the Australian monsoon

Analysis of cuttings from industry well West Tryal Rocks-1 (adjacent to Site NWS-4A) indicates that recovery of a >4 Ma upper slope record of climate variability and monsoon history is achievable (Fig. **F7**). Cores recovered during Expedition 356 provide the potential to generate a record comparable to other global climate proxy records. High core recovery will be necessary to achieve this and other objectives fully (see **"Risks and contingency"**); however, even partial core recovery will improve our understanding of the Australian monsoon prior to 1 Ma.

Most global climate proxy records are from the deep ocean basins, but one benefit of coring in a continental-margin setting is that the pollen is likely to be more abundant, delivered by fluvial outflow during the rainy season (van der Kaars and De Deckker, 2003). In comparison, pollen in deep-ocean cores relies on eolian delivery and is consequently less abundant. The Expedition 356 sites are also close to the southern edge of Australian monsoonal influence and can therefore be used to chart its latitudinal variability. Studies on pollen content in modern NWS marine sediments have concluded that the bioclimatic zones of the adjacent Australian continent are extremely well represented (van der Kaars and De Deckker, 2003). We also anticipate good pollen preservation in the Pliocene–Pleistocene interglacials at the shelfal sites and where mudstones/marls are most common in the Pliocene sections.

Little is known about the timing of the development of the characteristic synoptic-scale division of Australia into a winter-wet south and summer-wet north. At a first approximation, the intensity and timing of the monsoonal northern Australia dry seasons and frontal-dominated southern Australia are both controlled by the intensity and seasonal migration of the subtropical anticyclone. Hence, the history of the southern subtropical anticyclone may be critical to our understanding of the evolution of synoptic systems at both ends of the continent. However, it is unknown whether the late Neogene evolution of the Australian monsoon was synchronized with contemporaneous climatic evolution in the southern part of the continent. Nevertheless, the timing of patterns seen in the gamma maxima of the NWS (Fig. **F5**) shows similarities with data from southeastern Australia. For example, fossil insect and pollen analyses from a small upland paleolake in southeastern Australia indicate that high annual and summer rainfall persisted there until at least 1.5 Ma (Sniderman et al., 2009, 2013), which is inconsistent with the modern climates and vegetation patterns. Drying of a megalake in what is now the semi-arid interior of southeastern Australia did not occur until the early Pleistocene (1.5–1.4 Ma; McLaren and Wallace, 2010; McLaren et al., 2011, 2012, 2014), just when the NWS gamma profile becomes subdued (arrow on Fig. **F5**). In central Australia, there is evidence that the final phase of aridification, marked by the presence of active dune fields, did not initiate until ~1 Ma (Fujioka and Chappell, 2010). Hence, it is possible that the onset of modern patterns of rainfall seasonality across the continent, as well as the initiation of full aridity in inland Australia, were synchronized. Coring will provide new data to constrain our understanding of Southern Hemisphere Pleistocene climate evolution across a tropical to temperate gradient by including both the monsoonal sites (northern Sites NWS-1A to NWS-4A) and Site NWS-5A. Further insight into the relative input from precipitation can be obtained by analyzing the clay mineralogy of the marly facies (Gingele

et al., 2001a, 2001b). The percent kaolinite/illite/chlorite content in each horizon will vary depending on the relative intensity of precipitation and runoff from the source coastal hinterland. For example, reduced chlorite associated with a decrease in kaolinite is interpreted to indicate arid conditions on the NWS during the Holocene (Gingele et al., 2001a). In addition, geochemical analyses of dust in NWS sediments can be used as a relative aridity index (Stuut et al., 2014). Geochemical and foraminiferal proxy analyses at all sites may show paleoproductivity maxima and their possible relationship to the Australian monsoon and the position of the ITCZ. Particularly at upper slope Site NWS-4A, microfossil paleoproductivity analyses might also reveal the dominance of the West Australian Current over the Leeuwin Current during glacial periods (cf. Spooner et al., 2011) when the Australian monsoon is thought to have been weak. Site NWS-5A (~28°C) is located at the northern edge of the modern, winter rainfall–dominated regime of southwestern Australia. It is therefore ideally located to chart the onset of the mid-latitude, westerly wind regime that drives this winter-dominated precipitation regime through analysis of characteristic pollen assemblages.

Turney et al. (2006) suggested that late Quaternary climatic variability across northern Australia probably reflected changes in the latitude of the ITCZ, the westerlies, and ocean masses. However, these authors stated that "few local records are available that enable the frequency, timing, and latitudinal span to be reconstructed with great confidence." They note that biological or geomorphic proxy evidence might often show a time-transgressive response to climatic variability. They concluded with a plea to perform quantitative reconstructions of past climates in this region with a refined chronology. Recent biodiversity studies emphasize the uniqueness of the Australian monsoon biota (Oliver et al., 2014; Crisp and Cook, 2013) as it evolved in response to the changing monsoon and increased aridity in the Neogene. These authors acknowledge that not only are climate records of the Australian monsoon sparse, but there are also disagreements as to its timing. Thus, coring long well-constrained climate archives in the NWS will greatly enhance our understanding of the evolution and biogeography of the diverse biota of northern Australia.

3. Provide empirical input into the spatiotemporal patterns of subsidence along the NWS that can be used to place fundamental constraints on the interaction between Australian plate motion and mantle convection and to groundtruth geodynamic models.

Lateral displacements of continents relative to mantle convection patterns have significant impact on the flooding history of continental platforms and margins (Sleep, 1976; Gurnis, 1990, 1993; Russell and Gurnis, 1994). Eustatic curves constructed from

data from a single margin are known to misrepresent actual global sea levels because of the influence of dynamic topography (Müller et al., 2008b; Spasojević et al., 2008; Moucha et al., 2008). Since the breakup and dispersal of eastern Gondwana during the Cretaceous, the Australian plate has moved several thousand kilometers northward (Fig. **F8**) and recorded anomalous flooding patterns that cannot be reconciled with known eustatic variations (Fig. **F9**) (Russell and Gurnis 1994; Gurnis et al., 1998; Veevers, 2000; DiCaprio et al., 2009; Heine et al., 2010). Apart from these continental-scale observations, measurements of the amplitude, wavelength, and rate of dynamic topography resulting from circulation within the convecting mantle are rare. Subsidence anomalies along the NWS are ideal targets for investigation of dynamic topography, as the region lies across the gradient of the degree two geoid anomaly and on the fastest moving continent since the Eocene (about >35 Ma). These subsidence anomalies have long been known (Müller et al., 2000; Kennard et al., 2003) and can be ascribed to dynamic topography because both thermal subsidence and flexural effects are minimal (Czarnota et al., 2013).

Cooling of the lithospheric mantle as it returns to its pre-rift thickness drives post-rift thermal subsidence. As the final rifting phase on the NWS occurred more than 130 Ma, the lithospheric mantle should have completed re-thickening by the Neogene, and therefore thermal subsidence should have been insignificant during the Neogene and Quaternary. Flexural effects are likely to be negligible for two reasons. First, our sites are positioned beyond the ~200 km flexural response wavelength of plate boundaries. Secondly, the present elastic thickness of the NWS is ~5 km and therefore loads approach Airy isostasy (Fowler and McKenzie, 1989).

In the last five years, advancements in computer modeling have attributed subsidence anomalies along the NWS to dynamic drawdown of the Earth's surface driven by Australia's rapid northward motion over a generally stationary accumulation of subducted slabs within the mantle beneath southeast Asia (Lithgow-Bertelloni and Gurnis, 1997; Heine et al., 2010). These models predict that the NWS should be affected by a southward-propagating wave of subsidence related to Australia's northward motion over this stationary cold and dense mantle anomaly. Because Australia's northward motion is ~70 km/m.y. and the proposed drill sites span 10° of latitude, this model predicts a resolvable subsidence diachroneity of >10 m.y. between the northernmost and southernmost proposed drill sites.

In contrast to the diachronous results suggested by geodynamic modeling, recent backstripping of NWS clinoform rollover positions indicates that margin-wide anom-

alous subsidence was instead broadly synchronous and commenced ~10 Ma, with a down-to-the-north gradient equal in amplitude to adjacent oceanic floor residual depth anomalies (Czarnota et al., 2013). These data suggest that the mantle anomaly responsible for this subsidence may be transient and coupled to the plate motion. However, there is a lack of temporal resolution between 0-5 Ma because there are no well-defined clinoform rollovers of this age. Accurate, high-temporal-resolution subsidence analyses can directly resolve the discrepancy between the two end-member scenarios presented here, thereby providing fundamental insight into the interplay between plate motion and mantle convection.

Tectonic subsidence

Neogene and Quaternary subsidence histories for the NWS can be constructed with unprecedented accuracy using the Expedition 356 primary sites. To compare subsidence histories between drilling locations, 1-D water-loaded basement subsidence histories will be calculated assuming Airy isostasy. Flexural backstripping can also be performed because of the abundance of industry seismic profiles near the sites, but the low flexural rigidity of the region renders this degree of complexity unnecessary. Accurate knowledge of paleobathymetry, sediment compaction parameters, and lithology are essential for 0–5 Ma. In addition, the compaction parameters, lithology, and thickness of underlying sedimentary units are also needed because a large component of the accommodation space on passive margins results from the compaction of underlying sediments. Fortunately, the petroleum industry, government, and academia have extensively studied the underlying sediment pile and therefore the necessary data exist.

Paleobathymetric estimates

Paleobathymetry from foraminiferal and facies analyses is an essential input to backstripping analyses and is necessary to estimate relative sea level variations. Benthic assemblages, planktonic percentage, and sedimentary facies data may all be used to interpret paleodepths. Modern shelfal foraminiferal assemblages on Australia's continental margin are similar to Pliocene–Pleistocene assemblages and can therefore be used as modern analogs for paleodepth and paleonutrient interpretations (Smith and Gallagher, 2003; Smith et al., 2001). Modern benthic foraminiferal assemblage analog data from across the region may be used for this purpose, including Sunda Shelf (5°N to 10°N) (Biswas, 1976), Banda Sea and Timor Trough (5°S to 10°S) (van Marle, 1988), Sahul Shelf and Timor Sea (8°S to 14°S) (Loeblich and Tappan, 1994), Exmouth Gulf (22°S) (Haig, 1997; Orpin et al., 1999), Ningaloo Reef (24.48°S) (Parker, 2009), and the

western Australian continental shelf (20°S to 34°S) (Li et al., 1999; Betjeman, 1969; Quilty, 1977). These benthic foraminiferal assemblage analog data may be enhanced with paleodepth estimates from larger foraminifer distributions (Renema, 2006; James et al., 1999; Hohenegger, 1995; Langer and Hottinger, 2000; Hohenegger, 2005). The percentage of planktonic foraminifers in total assemblage data can also be used to estimate paleodepths (van der Zwaan et al., 1990) and has been used to obtain paleobathymetric estimates prior to backstripping and generation of subsidence curves (van Hinsbergen et al., 2005; Gallagher et al., 2013). Furthermore, paleoenvironmental analyses of ostracod assemblages may complement these analyses (Reeves et al., 2007). This holistic approach can be enhanced by interpretations of facies distributions (e.g., in situ ooid distribution) to generate robust paleobathymetric inputs into subsidence models.

Drilling and coring strategy

Previous work by both academia and industry on the NWS has provided abundant site data, including well completion reports, seismic data, wireline logs, cuttings, (rare) sidewall cores, and limited engineering cores in the latest Quaternary sections. Using these data, we identified a 10° latitudinal transect to investigate tropical reef and carbonate diachroneity related to Leeuwin Current intensity and ITF/Indo-Pacific Warm Pool influence.

Primary Sites NWS-1A, NWS-3A, NWS-4A, and NWS-6A (and corresponding alternate Sites NWS-7A, NWS-9A, NWS-10A, NWS-11A, and NWS-13A) (Fig. **F1**) will reveal insights into the timing and onset of reef development and are important targets because the pre-late Quaternary history of tropical reef development on the NWS is poorly known. The shelfal sites (all except Site NWS-4A) should allow us to obtain biogeographic evidence of ITF connectivity (Fig. **F4**), yielding a downstream record of this important ocean gateway. These shelfal sites are also likely to yield ooids, and coring will hopefully reveal the maximum age for these enigmatic tropical indexes in the Indian Ocean. Knowing the temporal and spatial distribution of ooids in the NWS will also provide insight into regional aridity and Indian Ocean alkalinity, and these data can also be used as paleodepth indexes. The presence of bathymetrically diagnostic facies, such as larger and smaller benthic foraminifers, at these five sites should permit well-constrained subsidence histories across 10° latitude, allowing the detailed temporal history of dynamic subsidence of the northern Australian plate to be constructed for the first time.

All of the sites are likely to yield spores and pollen, particularly during interglacials, and therefore yield a record of climate change and improve our understanding of the timing and nature of aridification in northwestern Australia. Compared to the eolian-derived floral assemblages from deep oceanic sites, material recovered from the NWS, closer to the shoreline, should contain predominantly fluvial-derived assemblages that will contribute to a more realistic assessment of regional climate. In particular, two shelfal to upper slope targets (Sites NSW-4A and NSW-5A) should provide particularly important climate records. Site NWS-4A is designed to provide insight into the onset and dynamics of the Australian monsoon and its relationship to obliquity forcing. If fully recovered, this would represent a quantum increase in our understanding of this important climate system because previous studies in the region focused only on the last 200 k.y. Site NWS-5A is not likely to yield an orbital-scale climate record because of slope erosional processes (Figs. **AF4, AF5**); however, it will complement Site NWS-4A because it lies south of a climatic divide between the Australian monsoon–dominated northern area and the westerly wind-driven, winter rainfall–dominated southern area (Fig. **F2**). Site NWS-5A will therefore provide a Pliocene–Pleistocene record of onset and variability of the southern Australian winter rainfall–dominated regime.

Our drilling and coring strategy is similar for each of the six primary (and seven alternate) sites; our primary operations plan is summarized in Table **T2.** For operational efficiency, we intend to core the sites in sequence from south to north (Fig. **F1**). The IODP Environmental Protection and Safety Panel (EPSP) approved all of the sites except for alternate Site NWS-11A. This site is pending final approval following review of additional seismic data. Our coring strategy consists of advanced piston coring (APC) in three holes (A, B, and C) at each site to ~200 meters below seafloor (mbsf) or APC refusal. APC refusal is an estimated depth that is formation dependent. It is usually defined two ways: (1) a complete stroke (determined by standpipe pressure) is not achieved because of formation hardness or (2) excessive force (>100,000 lb) is required to pull the core barrel out of the formation because it is too cohesive. In cases where a full stroke with the 9.5 m APC is not achieved, the half-length APC (4.8 m) may be used to deepen APC refusal. The decision to use the half-length APC technique will be influenced by operational timing.

Additionally in Holes B and C, the total penetration depth will be increased beyond APC refusal using the extended core barrel (XCB) technique. At two of the primary sites (NWS-3A and NWS-4A) and four of the alternate sites (NWS-11A, NWS-10A,

NWS-9A, and NWS-7A), a fourth hole (D) will be required to reach the target depths using the rotary core barrel (RCB) system.

After coring is completed at each site, the final hole (C or D) will be conditioned, displaced with logging mud, and logged (see **"Downhole measurements strategy"**).

Downhole measurements strategy

Formation temperature measurements

While APC coring in Hole A, a series of formation temperature measurements using the advanced piston coring temperature tool (APCT-3) are planned. If deemed necessary, the Sediment Temperature Tool may be deployed for additional temperature measurements.

Core orientation

All APC cores will be oriented with the FlexIT tool and will use nonmagnetic core barrels as much as possible.

Downhole wireline logging

At the time of writing this *Scientific Prospectus*, the contract for providing wireline logging services is not yet in place, but anticipated usage of basic wireline logging tools is similar to those provided during the Integrated Ocean Drilling Program. Wireline logging is currently planned for the deepest hole at each of our primary sites (Hole C or D), but implementation will actually depend on hole conditions. The wireline logging plan aims to provide information on in situ formation properties (lithologies, structures, and petrophysics) and orbital-scale cyclicities.

Three standard IODP tool string configurations will be deployed: the triple combination (triple combo), Formation MicroScanner (FMS)-sonic, and Versatile Seismic Imager (VSI).

At each site, the first tool string deployed will be the triple combo, which measures density, neutron porosity, resistivity, and natural and spectral gamma ray, along with calipers. The caliper log provided by the density tool will allow an assessment of hole conditions and the potential for success of subsequent logging runs. The second run

will be the FMS-sonic and will record gamma ray, sonic velocity (for compressional and shear waves), and high-resolution electrical images. The compressional velocity logs will be combined with the density logs to generate synthetic seismograms for detailed seismic-log correlations. To calibrate the integration of well and seismic data, the third run in each hole will be a vertical seismic profile (VSP) recorded with the VSI, which requires the use of a seismic sound source. The expected spacing between stations is 25 m over the entire open interval of each hole logged. Spacing could be adjusted for specific targets or hole conditions. The seismic sound source used during the VSP survey will be subject to the IODP marine mammal policy, including daylight-only operation of the sound source, and may have to be postponed or canceled if certain policy conditions are not met. For more information on specific logging tools, please refer to **iodp.ldeo.columbia.edu/TOOLS_LABS/.**

Downhole measurements will be the only data available where core recovery is incomplete. Moreover, the data will provide common measurements for core-log integration (density, natural gamma radiation, and magnetic susceptibility) and establish the link between borehole and core features and reflectors on seismic profiles by synthetic seismograms and VSP.

Risks and contingency

There are several risks to achieving the objectives of this expedition as it involves an ambitious coring plan. For example, all of our sites are located in shallow water (<220 m water depth), so special precautions are required to ensure the safety of the crew and equipment. In particular, sea state and the resulting heave behavior of the ship as a result of weather conditions are critical. Additionally, the nature of the sediments could negatively impact coring/logging operations, hole stability, core recovery and quality, and rate of penetration. A series of alternate sites are available for contingency operations (Table **T3**).

Sampling and data sharing strategy

Shipboard and shore-based researchers should refer to the IODP Sample, Data, and Obligations policy at **www.iodp.org/program-policies/.** This document outlines the policy for distributing IODP samples and data to research scientists, curators, and educators. The document also defines the obligations that sample and data recipients incur. The Sample Allocation Committee (SAC) (composed of co-chief scientists, staff

scientist, and IODP curator on shore and curatorial representative on board the ship) will work with the entire scientific party to formulate a formal expedition-specific sampling plan for shipboard and postcruise sampling.

Shipboard scientists are expected to submit postcruise research plans, including sample/data requests (at **http://web.iodp.tamu.edu/sdrm/**) no later than 3 months before the beginning of the expedition. This timing is necessary to coordinate the research to be conducted and to ensure that the scientific objectives are achieved. Based on sample requests (shore-based and shipboard), the SAC will prepare a tentative sampling plan. The sampling plan will be subject to modification depending upon the actual core recovery and collaborations that develop between scientists during the expedition. The SAC must approve modifications of the sampling strategy during the expedition.

All personal sample frequencies and sizes must be justified on a scientific basis and will depend on core recovery, the full spectrum of other sample requests, and the cruise objectives. Some redundancy of measurements is unavoidable, but minimizing the duplication of measurements among the shipboard party and identified shore-based collaborators will be a factor in evaluating sample requests. All shipboard scientists and approved shore-based requesters are expected to collaborate and cooperate within the framework of this plan. Sampling for individual scientist's postcruise research will completely depend on core recovery and may either take place on the ship or be deferred until after the cruise. This decision will be made during the expedition when core recovery and quality are better known.

Following Expedition 356, cores will be delivered to the IODP Core Repository at Kochi, Japan. All collected data and samples will be protected by a 1 y moratorium during which time they are available only to the Expedition 356 science party and approved shore-based participants. This moratorium will extend 1 y following either the end of the expedition or the completion of a postcruise sampling party, if required.

References

An, Z., 2000. The history and variability of the east Asian paleomonsoon climate. *Quaternary Science Review,* 19(1–5):171–187. **http://dx.doi.org/10.1016/S0277-3791(99)00060-8**

Audley-Charles, M.G., Ballantyne, P.D., and Hall, R., 1988. Mesozoic-Cenozoic rift-drift sequence of Asian fragments from Gondwanaland. *Tectonophysics,* 155(1–4):317–330. **http://dx.doi.org/10.1016/0040-1951(88)90272-7**

Beaufort, L., van der Kaars, S., Bassinot, F.C., and Moron, V., 2010. Past dynamics of the Australian monsoon: precession, phase and links to the global monsoon concept. *Climate of the Past,* 6(5):695–706. **http://dx.doi.org/10.5194/cp-6-695-2010**

Betjeman, K.J., 1969. Recent foraminifera from the western continental shelf of Western Australia. *Contributions from the Cushman Foundation for Foraminiferal Research,* 20(4):119–138.

Biswas, B., 1976. Bathymetry of Holocene foraminifera and Quaternary sea-level changes on the Sunda Shelf. *Journal of Foraminiferal Research,* 6(2):107–133. **http://dx.doi.org/10.2113/gsjfr.6.2.107**

Boote, D.R.D., and Kirk, R.B., 1989. Depositional wedge cycles on an evolving plate margin, western and northwestern Australia. *AAPG Bulletin,* 73(2):216–243.

Bosence, D., 2009. Carbonates, warm water. *In* Gornitz, V. (Ed.), *Encyclopedia of Paleoclimatology and Ancient Environments:* Dordrecht (Springer), 143–148.

Bowman, D.M.J.S., Brown, G.K., Braby, M.F., Brown, J.R., Cook, L.G., Crisp, M.D., Ford, F., Haberle, S., Hughes, J., Isagi, Y., Joseph, L., McBride, J., Nelson, G., and Ladiges, P.Y., 2010. Biogeography of the Australian monsoon tropics. *Journal of Biogeography,* 37(2):201–216. **http://dx.doi.org/10.1111/j.1365-2699.2009.02210.x**

Braithwaite, C.J.R., 1994. Quaternary oolites in the Indian Ocean. *Atoll Research Bulletin,* 420. **http://dx.doi.org/10.5479/si.00775630.420.1**

Carter, R.M., and Gammon, P., 2004. New Zealand maritime glaciation: millennial-scale southern climate change since 3.9 Ma. *Science,* 304(5677):1659–1662. **http://dx.doi.org/10.1126/science.1093726**

Cathro, D.L., Austin, J.A., Jr., and Moss, G.D., 2003. Progradation along a deeply submerged Oligocene–Miocene heterozoan carbonate shelf: how sensitive are clinoforms to sea level variations? *AAPG Bulletin,* 87(10):1547–1574. **http://dx.doi.org/10.1306/05210300177**

Clarke, J.D.A., 2009. Carbonates, cool water. *In* Gornitz, V. (Ed.), *Encyclopedia of Paleoclimatology and Ancient Environments:* Dordrecht (Springer), 138–143.

Collins, L.B., 2002. Tertiary foundations and Quaternary evolution of coral reef systems of Australia's North West Shelf. *In* Keep, M., and Moss, S.J. (Eds.), *The Sedimentary Basins of Western Australia* (Vol. 3): Perth (Petroleum Exploration Society of Australia), 129–152.

Collins, L.B., and Testa, V., 2010. Quaternary development of resilient reefs on the subsiding Kimberley continental margin, Northwest Australia. *Brazilian Journal of Oceanography,* 58(SPE1):67–77. **http://dx.doi.org/10.1590/S1679-87592010000500007**

Collins, L.B., Zhao, J.-X., and Freeman, H., 2006. A high-precision record of mid–late Holocene sea-level events from emergent coral pavements in the Houtman Abrolhos Islands, southwest Australia. *Quaternary International,* 145–146:78–85. **http://dx.doi.org/10.1016/j.quaint.2005.07.006**

Collins, L.B., Zhu, Z.R., Wyrwoll, K.-H., Hatcher, B.G., Playford, P.E., Eisenhauer, A., Chen, J.H., Wasserburg, G.J., and Bonani, G., 1993. Holocene growth history of a reef complex on a cool-water carbonate margin: Easter Group of the Houtman Abrolhos, Eastern

Indian Ocean. *Marine Geology,* 115(1–2):29–46. **http://dx.doi.org/10.1016/0025-3227(93)90073-5**

Cresswell, G.R., 1991. The Leeuwin Current: observations and recent models. *Journal of the Royal Society of Western Australia,* 74:1–14.

Crisp, M.D. and Cook, L.G., 2013. How was the Australian flora assembled over the last 65 million years? A molecular perspective. *Annual Review of Ecology, Evolution, and Systematics,* 44(1):303–324. **http://dx.doi.org/10.1146/annurev-ecolsys-110512-135910**

Czarnota, K., Hoggard, M.J., White, N., and Winterbourne, J., 2013. Spatial and temporal patterns of Cenozoic dynamic topography around Australia. *Geochemistry, Geophysics, Geosystems,* 14(3):634–658. **http://dx.doi.org/10.1029/2012GC004392**

Davies, G.R., 1970. Carbonate bank sedimentation, eastern Shark Bay, Western Australia. *In* Logan, B.W., Davies, G.R., Read, J.F., and Cebulski, D.E. (Eds.), *Carbonate Sedimentation and Environments, Shark Bay, Western Australia*. AAPG Memoir, 13:85–168. **http://archives.datapages.com/data/specpubs/carbona1/images/a040/a0400001/0050/00850.pdf**

de Garidel-Thoron, T., Rosenthal, Y., Bassinot, F., and Beaufort, L., 2005. Stable sea surface temperatures in the western Pacific warm pool over the past 1.75 million years. *Nature,* 433(7023):294–298. **http://dx.doi.org/10.1038/nature03189**

deMenocal, P.B., Bristow, J.F., and Stein, R., 1992. Paleoclimatic applications of downhole logs: Pliocene–Pleistocene results from Hole 798B, Sea of Japan. *In* Pisciotto, K.A., Ingle, J.C., Jr., von Breymann, M.T., Barron, J., et al., *Proceedings of the Ocean Drilling Program, Scientific Results,* 127/128 (Pt. 1): College Station, TX (Ocean Drilling Program), 393–406. **http://dx.doi.org/10.2973/odp.proc.sr.127128-1.143.1992**

DiCaprio, L., Gurnis, M., and Müller, R.D., 2009. Long-wavelength tilting of the Australian continent since the Late Cretaceous. *Earth and Planetary Science Letters,* 278(3–4):175–185. **http://dx.doi.org/10.1016/j.epsl.2008.11.030**

Driscoll, N.W., and Karner, G.D., 1998. Lower crustal extension across the northern Carnarvon Basin, Australia: evidence for an eastward dipping detachment. *Journal of Geophysical Research: Solid Earth,* 103(B3):4975–4991. **http://dx.doi.org/10.1029/97JB03295**

Dyksterhuis, S., Müller, R.D., and Albert, R.A., 2005. Paleostress field evolution of the Australian continent since the Eocene. *Journal of Geophysical Research: Solid Earth,* 110(B5):B05102. **http://dx.doi.org/10.1029/2003JB002728**

Ehrenberg, S.N., McArthur, J.M., and Thirlwall, M.F., 2006. Growth, demise, and dolomitization of Miocene carbonate platforms on the Marion Plateau, offshore NE Australia. *Journal of Sedimentary Research,* 76:91–116. **http://dx.doi.org/10.2110/jsr.2006.06**

Etheridge, M.A., and O'Brian, G.W., 1994. Structural and tectonic evolution of the Western Australian margin basin system. Petroleum Exploration Society of Australia Journal, 22:45–63.

Exon, N.F., and Colwell, J.B., 1994. Geological history of the outer North West Shelf of Australia: a synthesis. *AGSO Journal of Australian Geology and Geophysics,* 15(1):177–190.

Fowler, S., and McKenzie, D., 1989. Gravity studies of the Rockall and Exmouth Plateaux using SEASAT altimetry. *Basin Research,* 2(1):27–34. **http://dx.doi.org/10.1111/j.1365-2117.1989.tb00024.x**

Fujioka, T., and Chappell, J., 2010. History of Australian aridity: chronology in the evolution of landscapes. *Geological Society Special Publication,* 346(1):121–139 **http://dx.doi.org/10.1144/SP346.8**

Gallagher, S.J., Wallace, M.W., Li, C.L., Kinna, B., Bye, J.T., Akimoto, K., and Torii, M., 2009. Neogene history of the West Pacific Warm Pool, Kuroshio and Leeuwin Currents. *Paleoceanography,* 24(1):PA1206. **http://dx.doi.org/10.1029/2008PA001660**

Gallagher, S.J., Villa, G., Drysdale, R.N., Wade, B.S., Scher, H., Li, Q., Wallace, M.W., and Holdgate, G.R., 2013. A near-field sea level record of East Antarctic Ice Sheet instability from 32 to 27 Myr. *Paleoceanography,* 28(1):1–13. **http://dx.doi.org/10.1029/2012PA002326**

Gallagher, S.J., Wallace, M.W., Hoiles, P.W., and Southwood, J.M., in press. Seismic and stratigraphic evidence for reef expansion and onset of aridity on the Northwest Shelf of Australia during the Pleistocene. *Marine and Petroleum Geology*. **http://dx.doi.org/10.1016/j.marpetgeo.2014.06.011**

Gentilli, J., 1972. *Australian Climate Patterns:* Melbourne (Thomas Nelson).

Gingele, F.X., De Deckker, P., and Hillenbrand, C.-D., 2001a. Late Quaternary fluctuations of the Leeuwin Current and palaeoclimates on the adjacent landmasses: clay mineral evidence. *Australian Journal of Earth Sciences,* 48(6):867–874. **http://dx.doi.org/10.1046/j.1440-0952.2001.00905.x**

Gingele, F.X., De Deckker, P., and Hillenbrand, C.-D., 2001b. Clay mineral distribution in surface sediment between Indonesia and NW Australia—source and transport by ocean currents. *Marine Geology,* 179(3–4):135–146. **http://dx.doi.org/10.1016/S0025-3227(01)00194-3**

Goncharov, A., 2004. Basement and crustal structure of the Bonaparte and Browse Basins, Australian northwest margin. *In* Ellis, G., Baillie, P., and Munson, T. (Eds.), *Timor Sea Petroleum Geoscience, Proceedings of the Timor Sea Symposium*. Special Publication—Northern Territory Geological Survey, 551–566. **http://www.ga.gov.au/image_cache/GA8880.pdf**

Gordon, A.L., 2005. Oceanography of the Indonesian seas and their throughflow. *Oceanography,* 18(4):14–27. **http://dx.doi.org/10.5670/oceanog.2005.01**

Gradstein, F.M., Ogg, J.G., Schmitz, M.D., and Ogg, G.M. (Eds.)., 2012. *The Geological Time Scale 2012:* Amsterdam (Elsevier).

Greenstein, B.J., and Pandolfi, J.M., 2008. Escaping the heat: range shifts of reef coral taxa in coastal Western Australia. *Global Change Biology,* 14(3):513–528. **http://dx.doi.org/10.1111/j.1365-2486.2007.01506.x**

Greenwood, D.R., Herold, N., Huber, M., Müller, R.D., and Seton, M., 2012. Early to middle Miocene monsoon climate in Australia: reply. *Geology,* 40(6):e274. **http://dx.doi.org/10.1130/G33384Y.1**

Gurnis, M., 1990. Bounds on global dynamic topography from Phanerozoic flooding of continental platforms. *Nature,* 344(6268):754–756. **http://dx.doi.org/10.1038/344754a0**

Gurnis, M., 1993. Phanerozoic marine inundation of continents driven by dynamic topography above subducting slabs. *Nature,* 364(6438):589–593. **http://dx.doi.org/10.1038/364589a0**

Gurnis, M., Müller, R.D., and Moresi, L., 1998. Cretaceous vertical motion of Australia and the Australian–Antarctic Discordance. *Science,* 279(5356):1499–1504. **http://dx.doi.org/10.1126/science.279.5356.1499**

Haig, D.W., 1997. Foraminifera from Exmouth Gulf, Western Australia. *Journal of the Royal Society of Western Australia,* 80(4):263–280. **http://www.rswa.org.au/publications/Journal/80(4)/80(4)haig.pdf**

Hall, R., 2009. Southeast Asia's changing palaeogeography. *Blumea—Biodiversity, Evolution and Biogeography of Plants,* 54(1–3):148–161. **http://dx.doi.org/10.3767/000651909X475941**

Haq, B.U., and Al-Qahtani, A.M., 2005. Phanerozoic cycles of sea-level change on the Arabian Platform. *GeoArabia,* 10(2):127–160. **http://www.gulfpetrolink.net/mepr/dwnld/Haq-and-Al-Qahtani-2005/Haq_and_Qahtani_layout.pdf**

Haq, B.U., Hardenbol, J., and Vail, P.R., 1987. Chronology of fluctuating sea levels since the Triassic. *Science,* 235(4793):1156–1167. **http://dx.doi.org/10.1126/science.235.4793.1156**

Hearty, P., O'Leary, M., Donald, A., and Lachlan, T., 2006. The enigma of 3400 years BP coastal oolites in tropical northwest Western Australia... why then, why there? *Sedimentary Geology,* 186(3–4):171–185. **http://dx.doi.org/10.1016/j.sedgeo.2005.11.014**

Hearty, P.J., Webster, J.M., Clague, D.A., Kaufman, D.S., Bright, J., Southon, J., and Renema, W., 2010. A pulse of ooid formation in Maui Nui (Hawaiian Islands) during Termination I. *Marine Geology,* 268(1–4):152–162. **http://dx.doi.org/10.1016/j.margeo.2009.11.007**

Heine, C., and Müller, R.D., 2005. Late Jurassic rifting along the Australian North West Shelf: margin geometry and spreading ridge configuration. *Australian Journal of Earth Sciences,* 52(1):27–39. **http://dx.doi.org/10.1080/08120090500100077**

Heine, C., Müller, R.D., Steinberger, B., and DiCaprio, L., 2010. Integrating deep Earth dynamics in paleogeographic reconstructions of Australia. *Tectonophysics,* 483(1–2):135–150. **http://dx.doi.org/10.1016/j.tecto.2009.08.028**

Herold, N., Huber, M., Greenwood, D.R., Müller, R.D., and Seton, M., 2011. Early to middle Miocene monsoon climate in Australia. *Geology,* 39(1):3–6. **http://dx.doi.org/10.1130/G31208.1**

Hesse, P.P., Magee, J.W., and van der Kaars, S., 2004. Late Quaternary climates of the Australian arid zone: a review. *Quaternary International,* 118–119:87–102. **http://dx.doi.org/10.1016/S1040-6182(03)00132-0**

Hohenegger, J., 1995. Depth estimation by proportions of living larger foraminifera. *Marine Micropaleontology,* 26(1–4):31–47. **http://dx.doi.org/10.1016/0377-8398(95)00044-5**

Hohenegger, J., 2005. Estimation of environmental paleogradient values based on presence/absence data: a case study using benthic foraminifera for paleodepth estimation. *Palaeogeography, Palaeoclimatology, Palaeoecology,* 217(1–2):115–130. **http://dx.doi.org/10.1016/j.palaeo.2004.11.020**

Hoiles, P.W., Gallagher, S.J., Kitamura, A., and Southwood, J.M., 2012. The evolution of the Tsushima Current during the early Pleistocene in the Sea of Japan: an example from marine isotope stage (MIS) 47. *Global and Planetary Change*, 92–93:162–178. **http://dx.doi.org/10.1016/j.gloplacha.2012.05.015**

Holbourn, A., Kuhnt, W., Kawamura, H., Jian, Z., Grootes, P., Erlenkeuser, H., and Xu, J., 2005. Orbitally paced paleoproductivity variations in the Timor Sea and Indonesian Throughflow variability during the last 460 kyr. *Paleoceanography,* 20(3):PA3002. **http://dx.doi.org/10.1029/2004PA001094**

Huang, Y.-S., Lee, T.-Q., and Hsu, S.-K., 2011. Milankovitch-scale environmental variation in the Banda Sea over the past 820 ka: fluctuation of the Indonesian Throughflow intensity. *Journal of Asian Earth Sciences,* 40(6):1180–1188. **http://dx.doi.org/10.1016/j.jseaes.2010.08.011**

Hull, J.N.F., and Griffiths, C.M., 2002. Sequence stratigraphic evolution of the Albian to Recent section of the Dampier Sub-basin, North West Shelf, Australia. *In* Keep, M., and Moss, S.J. (Eds.), *The Sedimentary Basins of Western Australia* (Vol. 3): Perth (Petroleum Exploration Society of Australia), 617–639.

Isern, A.R., Langford, R.P., Truswell, E.M., and Wilford, G.E., 1995. Cainozoic. *In* Langford, R.P., Wilford, G.E., Truswell, E.M., and Isern, A.R. (Eds.), *Paleogeographic Atlas of Australia*

(Vol. 10): Canberra (Australian Geological Survey Organization). **http://www.ga.gov.au/meta/ANZCW0703003727.html**

James, N.P., and Bone, Y., 1991. Origin of a cool-water, Oligo–Miocene deep shelf limestone, Eucla Platform, southern Australia. *Sedimentology,* 38(2):323–341. **http://dx.doi.org/10.1111/j.1365-3091.1991.tb01263.x**

James, N.P., Bone, Y., Kyser, T.K., Dix, G.R., and Collins, L.B., 2004. The importance of changing oceanography in controlling late Quaternary carbonate sedimentation on a high-energy, tropical, oceanic ramp: north-western Australia. *Sedimentology,* 51(6):1179–1205. **http://dx.doi.org/10.1111/j.1365-3091.2004.00666.x**

James, N.P., Collins, L.B., Bone, Y., and Hallock, P., 1999. Subtropical carbonates in a temperate realm; modern sediments on the southwest Australian shelf. *Journal of Sedimentary Research,* 69(6):1297–1321. **http://dx.doi.org/10.2110/jsr.69.1297**

Jian, Z., Yu, Y., Li, B., Wang, J., Zhang, X., and Zhou, Z., 2006. Phased evolution of the south–north hydrographic gradient in the South China Sea since the middle Miocene. *Palaeogeography, Palaeoclimatology, Palaeoecology,* 230(3–4):251–263. **http://dx.doi.org/10.1016/j.palaeo.2005.07.018**

Jones, H.A., 1973. *Marine geology of the Northwest Australian continental shelf.* (Bulletin—Bureau of Mineral Resources, Geology and Geophysics (Australia), 136. **http://www.ga.gov.au/corporate_data/104/Bull_136.pdf**

Karas, C., Nürnberg, D., Gupta, A.K., Tiedemann, R., Mohan, K., and Bickert, T., 2009. Mid-Pliocene climate change amplified by a switch in Indonesian subsurface throughflow. *Nature Geoscience,* 2(6):434–438. **http://dx.doi.org/10.1038/ngeo520**

Karas, C., Nürnberg, D., Tiedemann, R., and Garbe-Schönberg, D., 2011. Pliocene Indonesian Throughflow and Leeuwin Current dynamics: implications for Indian Ocean polar heat flux. *Paleoceanography,* 26(2):PA2217. **http://dx.doi.org/10.1029/2010PA001949**

Kawamura, H., Holbourn, A., and Kuhnt, W., 2006. Climate variability and land–ocean interactions in the Indo Pacific Warm Pool: a 460-ka palynological and organic geochemical record from the Timor Sea. *Marine Micropaleontology,* 59(1):1–14. **http://dx.doi.org/10.1016/j.marmicro.2005.09.001**

Kendrick, G.W., Wyrwoll, K.-H., and Szabo, B.J., 1991. Pliocene–Pleistocene coastal events and history along the western margin of Australia. *Quaternary Science Reviews,* 10(5):419–439. **http://dx.doi.org/10.1016/0277-3791(91)90005-F**

Kennard, J.M., Deighton, I., Ryan, D., Edwards, D.S., and Boreham, C.J., 2003. Subsidence and thermal history modelling: new insights into hydrocarbon expulsion from multiple petroleum systems in the Browse Basin. *In* Ellis, G.K., Baillie, P.W., and Munson, T.J. (Eds.), *Proceedings of the Timor Sea Symposium:* Northern Territory Geological Survey—Special Publication, 1:411–435.

Kennett, J.P., Keller, G., and Srinivasan, M.S., 1985. Miocene planktonic foraminiferal biogeography and paleoceanographic development of the Indo-Pacific region. *In* Kennett, J.P. (Ed.), *The Miocene Ocean: Paleoceanography and Biogeography.* Memoir—Geological Society of America, 163:197–236. **http://dx.doi.org/10.1130/MEM163-p197**

Kershaw, A.P., van der Kaars, S., and Moss, P.T., 2003. Late Quaternary Milankovitch-scale climatic change and variability and its impact on monsoonal Australasia. *Marine Geology,* 201(1–3):81–95. **http://dx.doi.org/10.1016/S0025-3227(03)00210-X**

Kleypas, J.A., McManus, J.W., and Meñez, L.A.B., 1999. Environmental limits to coral reef development: where do we draw the line? *Integrative and Comparative Biology,* 39(1):146–159. **http://dx.doi.org/10.1093/icb/39.1.146**

Kominz, M.A., Browning, J.V., Miller, K.G., Sugarman, P.J., Misintseva, S., and Scotese, C.R., 2008. Late Cretaceous to Miocene sea-level estimates from the New Jersey and Delaware coastal plain coreholes: an error analysis. *Basin Research,* 20(2):211–226. **http://dx.doi.org/10.1111/j.1365-2117.2008.00354.x**

Kuhnt, W., Holbourn, A., Hall, R., Zuvela, M. and Käse, R., 2004. Neogene history of the Indonesian throughflow. *In* Clift, P., Wang, P., Kuhnt, W., and Hayes, D. (Eds.), *Continent-Ocean Interactions within East Asian Marginal Seas*. Geophysical Monograph, 149:299–320. **http://dx.doi.org/10.1029/149GM16**

Langer, M.R., and Hottinger, L., 2000. Biogeography of selected "larger" foraminifera. *Micropaleontology,* 46(Suppl. 1):105–126. **http://www.jstor.org/stable/1486184**

Lee, T.-Y., and Lawver, L.A., 1995. Cenozoic plate reconstruction of Southeast Asia. *Tectonophysics,* 251(1–4): 85–138. **http://dx.doi.org/10.1016/0040-1951(95)00023-2**

Lees, A., and Buller, A.T., 1972. Modern temperate-water and warm-water shelf carbonate sediments contrasted. *Marine Geology,* 13(5):M67–M73. **http://dx.doi.org/10.1016/0025-3227(72)90011-4**

Li, Q., James, N.P., Bone, Y., and McGowran, B., 1999. Palaeoceanographic significance of Recent foraminiferal biofacies on the southern shelf of Western Australia: a preliminary study. *Palaeogeography, Palaeoclimatology, Palaeoecology,* 147(1–2):101–120. **http://dx.doi.org/10.1016/S0031-0182(98)00150-3**

Lisiecki, L.E., and Raymo, M.E., 2005. A Pliocene–Pleistocene stack of 57 globally distributed benthic $\delta^{18}O$ records. *Paleoceanography,* 20(1):PA1003. **http://dx.doi.org/10.1029/2004PA001071**

Lithgow Bertelloni, C., and Gurnis, B., 1997. Cenozoic subsidence and uplift of continents from time-varying dynamic topography. *Geology,* 25(8):735–738. **http://dx.doi.org/10.1130/0091-7613(1997)025<0735:CSAUOC>2.3.CO;2**

Liu, C., Fulthorpe, C.S., Austin, J.A., Jr., and Sanchez, C.M., 2011. Geomorphologic indicators of sea level and lowstand paleo-shelf exposure on early–middle Miocene sequence boundaries. *Marine Geology,* 208(1–4):179–191. **http://dx.doi.org/10.1016/j.margeo.2010.12.010**

Loeblich, A.R., Jr., and Tappan, H., 1994. Foraminifera of the Sahul shelf and Timor Sea. *Special Publication Cushman Foundation for Foraminiferal Research,* 31.

Longley, I.M., Buessenschuett, C., Clydsdale, L., Cubitt, C.J., Davis, R.C., Johnson, M.K., Marshall, N.M., Murray, A.P., Somerville, R., Spry, T.B., and Thompson, N.B., 2002. The north west shelf of Australia—a Woodside perspective. *In* Keep, M., and Moss, S.J. (Eds.), *The Sedimentary Basins of Western Australia* (Vol. 3): Perth (Petroleum Exploration Society of Australia), 27–88.

Magee, J.W., Miller, G.H., Spooner, N.A., and Questiaux, D., 2004. Continuous 150 k.y. monsoon record from Lake Eyre, Australia: insolation-forcing implications and unexpected Holocene failure. *Geology,* 32(10):885–888. **http://dx.doi.org/10.1130/G20672.1**

Malcolm, R.J., Pott, M.C., and Delfos, E., 1991. A new tectono-stratigraphic synthesis of the North West Cape area. *APPEA Journal,* 31(1):154–176.

Martin, H.A., and McMinn, A., 1994. Late Cainozoic vegetation history of north-western Australia, from the palynology of a deep sea core (ODP Site 765). *Australian Journal of Botany,* 42(1):95–102. **http://dx.doi.org/10.1071/BT9940095**

McClymont, E.L., Sosdian, S.M., Rosell-Melé, A., and Rosenthal, Y., 2013. Pleistocene sea-surface temperature evolution: early cooling, delayed glacial intensification, and implica-

tions for the mid-Pleistocene climate transition. *Earth-Science Review,* 123:173–193. **http://dx.doi.org/10.1016/j.earscirev.2013.04.006**

McGowran, B., Li, Q., Cann, J., Padley, D., McKirdy, D.M., and Shafik, S., 1997. Biogeographic impact of the Leeuwin Current in southern Australia since the late middle Eocene. *Palaeogeography, Palaeoclimatology, Palaeoecology,* 136(1–4):19–40. **http://dx.doi.org/10.1016/S0031-0182(97)00073-4**

McLaren, S., and Wallace, M.W., 2010. Plio–Pleistocene climate change and the onset of aridity in southeastern Australia. *Global and Planetary Change,* 71(1–2):55–72. **http://dx.doi.org/10.1016/j.gloplacha.2009.12.007**

McLaren, S., Wallace, M.W., Gallagher, S.J., Miranda, J.A., Holdgate, G.R., Gow, L.J., Snowball, I., and Sandgren, P., 2011. Palaeogeographic, climatic and tectonic change in southeastern Australia: the late Neogene evolution of the Murray Basin. *Quaternary Science Reviews,* 30(9–10):1086–1111. **http://dx.doi.org/10.1016/j.quascirev.2010.12.016**

McLaren, S., Wallace, M.W., Gallagher, S.J., Wagstaff, B.E., and Tosolini, A.-M.P., 2014. The development of a climate: an arid continent with wet fringes. *In* Prins, H.H.T., and Gordon, I.J. (Eds.), *Invasion Biology and Ecosystem Theory: Insights from a Continent in Transformation:* Cambridge (Cambridge University Press), 256–280.

McLaren, S., Wallace, M.W., and Reynolds, T., 2012. The late Pleistocene evolution of palaeo megalake Bungunnia, southeastern Australia: a sedimentary record of fluctuating lake dynamics, climate change and the formation of the modern Murray River. *Palaeogeography, Palaeoclimatology, Palaeoecology,* 317–318:114–127. **http://dx.doi.org/10.1016/j.palaeo.2011.12.020**

McMinn, A., 1992. Neogene dinoflagellate distribution in the eastern Indian Ocean from Leg 123, Site 765. *In* Gradstein, F.M., Ludden, J.N., et al., *Proceedings of the Ocean Drilling Program, Scientific Results,* 123: College Station, TX (Ocean Drilling Program), 429–441. **http://dx.doi.org/10.2973/odp.proc.sr.123.120.1992**

McMinn, A., 2002. Marine Quaternary dinoflagellate cysts of Australia, Papua-New Guinea, New Zealand and the Southern Ocean: a review. *Alcheringa,* 26(4):519–530. **http://dx.doi.org/10.1080/03115510208619541**

McMinn, A., and Martin, H., 1992. Late Cenozoic pollen history from Site 765, eastern Indian Ocean. *In* Gradstein, F.M., Ludden, J.N., et al., *Proceedings of the Ocean Drilling Program, Scientific Results,* 123: College Station, TX (Ocean Drilling Program), 421–427. **http://dx.doi.org/10.2973/odp.proc.sr.123.166.1992**

Metcalfe, I., 1988. Origin and assembly of south-east Asian continental terranes. *In* Audley-Charles, M.G., and Hallam, A. (Eds.), *Gondwana and Tethys*. Geological Society Special Publication, 37(1):101–118. **http://dx.doi.org/10.1144/GSL.SP.1988.037.01.08**

Miller, K.G., Kominz, M.A., Browning, J.V., Wright, J.D., Mountain, G.S., Katz, M.E., Sugarman, P.J., Cramer, B.S., Christie-Blick, N., and Pekar, S.F., 2005. The Phanerozoic record of global sea-level change. *Science,* 310(5752):1293–1298. **http://dx.doi.org/10.1126/science.1116412**

Moss, G.D., Cathro, D.L., and Austin, J.A., Jr., 2004. Sequence biostratigraphy of prograding clinoforms, northern Carnarvon Basin, Western Australia: a proxy for variations in Oligocene to Pliocene global sea level? *Palaios,* 19(3):206–226. **http://dx.doi.org/10.1669/0883-1351(2004)019<0206:SBOPCN>2.0.CO;2**

Moucha, R., Forte, A.M., Mitrovica, J.X., Rowley, D.B., Quéré, S., Simmons, N.A., and Grand, S.P., 2008. Dynamic topography and long-term sea-level variations: there is no such thing as a stable continental platform. *Earth and Planetary Science Letters,* 271(1–4):101–108. **http://dx.doi.org/10.1016/j.epsl.2008.03.056**

Müller, R.D., Lim, V.S.L., and Isern, A.R., 2000. Late Tertiary tectonic subsidence on the northeast Australian passive margin: response to dynamic topography? *Marine Geology,* 162(2–4):337–352. **http://dx.doi.org/10.1016/S0025-3227(99)00089-4**

Müller, R.D., Sdrolias, M., Gaina, C., and Roest, W.R., 2008a. Age, spreading rates, and spreading asymmetry of the world's ocean crust. *Geochemistry, Geophysics., Geosystems,* 9(4):Q04006. **http://dx.doi.org/10.1029/2007GC001743**

Müller, R.D., Sdrolias, M., Gaina, C., Steinberger, B., and Heine, C., 2008b. Long-term sea-level fluctuations driven by ocean basin dynamics. *Science,* 319(5868):1357–1362. **http://dx.doi.org/10.1126/science.1151540**

Oliver, P.M., Laver, R.J., Smith, K.L., and Bauer, A.M., 2014. Long-term persistence and vicariance within the Australian Monsoonal Tropics: the case of the giant cave and tree geckos (*Pseudothecadactylus*). *Australian Journal of Zoology,* 61(6):462–468. **http://dx.doi.org/10.1071/ZO13080**

Orpin, A.R., Haig, D.W., and Woolfe, K.J., 1999. Sedimentary and foraminiferal facies in Exmouth Gulf, in arid tropical northwestern Australia. *Australian Journal of Earth Sciences,* 46(4):607–621. **http://dx.doi.org/10.1046/j.1440-0952.1999.00728.x**

Parker, J.H., 2009. Taxonomy of foraminifera from Ningaloo Reef, Western Australia. *Memoirs of the Association of Australasian Palaeontologists*, 36.

Pattiaratchi, C., 2006. Surface and sub-surface circulation and water masses off Western Australia. *Bulletin of the Australian Meteorological and Oceanographic Society,* 19:95–104.

Pearce, A., 2009. Introduction: some historical "milestones" in the Leeuwin Current, and the Leeuwin Current Symposium 2007. *Journal of the Royal Society of Western Australia,* 92(2):31–36.

Quilty, P.G., 1977. Foraminifera of Hardy Inlet, southwestern Australia. *Journal of the Royal Society of Western Australia,* 59(3):79–90.

Rankey, E.C., and Reeder, S.L., 2009. Holocene ooids of Aitutaki Atoll, Cook Islands, South Pacific. *Geology,* 37(11):971–974. **http://dx.doi.org/10.1130/G30332A.1**

Reeves, J.M., Chivas, A.R., Garcia. A., and De Deckker, P., 2007. Palaeoenvironmental change in the Gulf of Carpentaria (Australia) since the last interglacial based on ostracoda. *Palaeogeography, Palaeoclimatology, Palaeoecology,* 246(2–4):163–187. **http://dx.doi.org/10.1016/j.palaeo.2006.09.012**

Renema, W., 2006. Large benthic foraminifera from the deep photic zone of a mixed siliciclastic-carbonate shelf off East Kalimantan, Indonesia. *Marine Micropaleontology,* 58(2):73–82. **http://dx.doi.org/10.1016/j.marmicro.2005.10.004**

Richardson, A.N., and Blundell, D.J., 1996. Continental collision in the Banda arc. *Geological Society Special Publication,* 106(1):47–60. **http://dx.doi.org/10.1144/GSL.SP.1996.106.01.05**

Rohling, E.J., Foster, G.L., Grant, K.M., Marino, G., Roberts, A.P., Tamisiea, M.E., and Williams, F., 2014. Sea-level and deep-sea-temperature variability over the past 5.3 million years. *Nature,* 508(7497):477–482. **http://dx.doi.org/10.1038/nature13230**

Romine, K.K., Durrant, J.M., Cathro, D.L., and Bernardel, G., 1997. Petroleum play element prediction for the Cretaceous–Tertiary basin phase, northern Carnarvon Basin. *APPEA Journal,* 37(1):315–338.

Rosleff-Soerensen, B., Reuning, L., Back, S., and Kukla, P., 2012. Seismic geomorphology and growth architecture of a Miocene barrier reef, Browse Basin, NW-Australia. *Marine and Petroleum Geology,* 29(1):233–254. **http://dx.doi.org/10.1016/j.marpetgeo.2010.11.001**

Russell, M., and Gurnis, M., 1994. The planform of epeirogeny: vertical motions of Australia during the Cretaceous. *Basin Research,* 6(2–3):63–76. **http://dx.doi.org/10.1111/j.1365-2117.1994.tb00076.x**

Ryan, G.J., Bernadel, G., Kennard, J.M., Jones, A.T., Logan, G.A., and Rollet, N., 2009. A precursor extensive Miocene reef system to the Rowley Shoals reefs, WA: evidence for structural control of reef growth or natural hydrocarbon seepage? *APPEA Journal,* 49:337–363.

Sakai, S., and Jige, M., 2006. Characterization of magnetic particles and magnetostratigraphic dating of shallow-water carbonates in the Ryukyu Islands, northwestern Pacific. *Island Arc,* 15(4):468–475. **http://dx.doi.org/10.1111/j.1440-1738.2006.00542.x**

Sayers, J., Symonds, P.A., Direen, N.G., and Bernardel, G., 2001. Nature of the continent–ocean transition on the non-volcanic rifted margin of the central Great Australian Bight. *In* Wilson, R.C.L., Whitmarsh, R.B., Taylor, B., and Froitzheim, N. (Eds.), *Non-volcanic Rifting of Continental Margins: A Comparison of Evidence from Land and Sea*. Geological Society Special Publication, 187(1):51–76. **http://dx.doi.org/10.1144/GSL.SP.2001.187.01.04**

Sengor, A.M.C., 1987. Tectonics of the Tethysides: orogenic collage development in a collisional setting. *Annual Review of Earth and Planetary Sciences,* 15(1):213–244. **http://dx.doi.org/10.1146/annurev.ea.15.050187.001241**

Simone, L., 1981. Ooids: a review. *Earth-Science Reviews,* 16:319–355. **http://dx.doi.org/10.1016/0012-8252(80)90053-7**

Sinha, D.K., Singh, A.K., and Tiwari, M., 2006. Palaeoceanographic and palaeoclimatic history of ODP Site 763A (Exmouth Plateau), southeast Indian Ocean: 2.2 Ma record of planktic foraminifera. *Current Science,* 90(10):1363–1369. **http://www.currentscience.ac.in/Downloads/article_id_090_10_1363_1369_0.pdf**

Sleep, N.H., 1976. Platform subsidence mechanisms and "eustatic" sea-level changes. *Tectonophysics,* 36(1–3):45–56. **http://dx.doi.org/10.1016/0040-1951(76)90005-6**

Smith, A.J., and Gallagher, S.J., 2003. The Recent foraminifera and facies of the Bass Canyon: a temperate submarine canyon in Gippsland, Australia. *Journal of Micropalaeontology,* 22(1):63–83. **http://dx.doi.org/10.1144/jm.22.1.63**

Smith, A.J., Gallagher, S.J., Wallace, M., Holdgate, G., Daniels, J., and Keene, J., 2001. The Recent temperate foraminiferal biofacies of the Gippsland Shelf: an analogue for Neogene environmental analyses in southeastern Australia. *Journal of Micropalaeontology,* 20(2):127–142. **http://dx.doi.org/10.1144/jm.20.2.127**

Sniderman J.M.K., Porch, N., and Kershaw, A.P., 2009. Quantitative reconstruction of early Pleistocene climate in southeastern Australia and implications for atmospheric circulation. *Quaternary Science Reviews,* 28(27–28):3185–3196. **http://dx.doi.org/10.1016/j.quascirev.2009.08.006**

Sniderman J.M.K., Jordan G.J., and Cowling, R.M., 2013. Fossil evidence for a hyperdiverse sclerophyll flora under a non-Mediterranean-type climate. *Proceedings of the National Academy of Sciences of the United States of America,* 110(9):3423–3428. **http://dx.doi.org/10.1073/pnas.1216747110**

Spasojević, S., Liu, L., Gurnis, M., and Müller, R.D., 2008. The case for dynamic subsidence of the U.S. east coast since the Eocene. *Geophysical Research Letters,* 35(8):L08305. **http://dx.doi.org/10.1029/2008GL033511**

Spooner, M.I., Barrows, T.T., De Deckker, P., and Paterne, M., 2005. Palaeoceanography of the Banda Sea, and late Pleistocene initiation of the northwest monsoon. *Global and Planetary Change,* 49(1–2):28–46. **http://dx.doi.org/10.1016/j.gloplacha.2005.05.002**

Spooner, M.I., De Deckker, P., Barrows, T.T., and Fifield, L.K., 2011. The behaviour of the Leeuwin Current offshore NW Australia during the last five glacial–interglacial cycles. *Global and Planetary Change,* 75(3–4):119–132. **http://dx.doi.org/10.1016/j.gloplacha.2010.10.015**

Srinivasan, M.S., and Sinha, D.K., 1998. Early Pliocene closing of the Indonesian Seaway: evidence from north-east Indian Ocean and tropical Pacific deep sea cores. *Journal of Asian Earth Sciences,* 16(1):29–44. **http://dx.doi.org/10.1016/S0743-9547(97)00041-X**

Struckmeyer, H.I.M., Blevin, J.E., Sayers, J., Totterdell, J.M., Baxter, K., and Cathro, D.L. 1998. Structural evolution of the Browse Basin, North West Shelf: new concepts from deep-seismic data. *In* Purcell, P.G., and Purcell, R.R. (Eds.), *The Sedimentary Basins of Western Australia* (Vol. 2): Perth (Petroleum Exploration Society of Australia), 345–368.

Sturman, A.P., and Tapper, N.J., 2005. *The Weather and Climate of Australia and New Zealand:* Melbourne (Oxford University Press).

Stuut, J.-B.W., Temmesfield, F., and De Deckker, P., 2014. A 550 ka record of aeolian activity near North West Cape, Australia: inferences from grain-size distributions and bulk chemistry of SE Indian Ocean deep-sea sediments. *Quaternary Science Reviews,* 83:83–94. **http://dx.doi.org/10.1016/j.quascirev.2013.11.003**

Suppiah, R., 1992. The Australian summer monsoon: a review. *Progress in Physical Geography,* 16(3):283–318. **http://dx.doi.org/10.1177/030913339201600302**

Tomczak, M., and Godfrey, J.S., 1994. *Regional Oceanography: An Introduction:* New York (Pergamon Press).

Turney, C.S.M., Haberle, S., Fink, D., Kershaw, A.P., Barbetti, M., Barrows, T.T., Black, M., Cohen, T.J., Corrège, T., Hesse, P.P., Hua, Q., Johnston, R., Morgan, V., Moss, P., Nanson, G., van Ommen, T., Rule, S., Williams, N.J., Zhao, J.-X., D'Costa, D., Feng, Y.-X., Gagan, M., Mooney, S., and Xia, Q., 2006. Integration of ice-core, marine and terrestrial records for the Australian Last Glacial Maximum and Termination: a contribution from the OZ INTIMATE group. *Journal of Quaternary Science,* 21(7):751–761. **http://dx.doi.org/10.1002/jqs.1073**

van der Kaars, S., and De Deckker, P., 2002. A late Quaternary pollen record from deep-sea Core Fr10/95, GC17 offshore Cape Range Peninsula, northwestern Western Australia. *Review of Palaeobotany and Palynology,* 120(1–2):17–39. **http://dx.doi.org/10.1016/S0034-6667(02)00075-1**

van der Kaars, S., and De Deckker, P., 2003. Pollen distribution in marine surface sediments offshore Western Australia. *Review of Palaeobotany and Palynology,* 124(1–2):113–129. **http://dx.doi.org/10.1016/S0034-6667(02)00250-6**

van der Kaars, S., De Deckker, P., and Gingele, F.X., 2006. A 100,000-year record of annual and seasonal rainfall and temperature for northwestern Australia based on a pollen record obtained offshore. *Journal of Quaternary Science,* 21(8):879–889. **http://dx.doi.org/10.1002/jqs.1010**

van der Zwaan, G.J., Jorissen, F.J., and de Stigter, H.C., 1990. The depth dependency of planktonic/benthic foraminiferal ratios: constraints and applications. *Marine Geology,* 95(1):1–16. **http://dx.doi.org/10.1016/0025-3227(90)90016-D**

van Hinsbergen, D.J.J., Kouwenhoven, T.J., and van der Zwaan, G.J., 2005. Paleobathymetry in the backstripping procedure: correction for oxygenation effects on depth estimates. *Palaeogeography, Palaeoclimatology, Palaeoecology,* 221(3–4):245–265. **http://dx.doi.org/10.1016/j.palaeo.2005.02.013**

van Marle, L.J., 1988. Bathymetric distribution of benthic foraminifera on the Australian-Irian Jaya continental margin, eastern Indonesia. *Marine Micropaleontology,* 13(2):97–152. **http://dx.doi.org/10.1016/0377-8398(88)90001-1**

Veevers, J.J. (Ed.), 2000. *Billion-Year Earth History of Australia and Neighbours in Gondwanaland:* Sydney (GEMOC Press, Macquarie University), 400.

Veevers, J.J., Powell, C.M., and Roots, S.R., 1991. Review of seafloor spreading around Australia. I. Synthesis of the patterns of spreading. *Australian Journal of Earth Sciences,* 38(4):373–389. **http://dx.doi.org/10.1080/08120099108727979**

von Rad, U., Haq, B.U., et al., 1992. *Proceedings of the Ocean Drilling Program, Scientific Results,* 122: College Station, TX (Ocean Drilling Program). **http://dx.doi.org/10.2973/odp.proc.sr.122.1992**

Wallace, M.W., Condilis, E., Powell, A., Redfearn, J., Auld, K., Wiltshire, M., Holdgate, G., and Gallagher, S., 2003. Geological controls on sonic velocity in the Cenozoic carbonates of the northern Carnarvon Basin, North West Shelf, Western Australia. *APPEA Journal,* 43(1):385–400.

Wallace, M.W., Holdgate, G.R., Daniels, J., Gallagher, S.J., and Smith, A., 2002. Sonic velocity, submarine canyons, and burial diagenesis in Oligocene–Holocene cool-water carbonates, Gippsland Basin, southeast Australia. *AAPG Bulletin,* 86(9):1593–1607. **http://dx.doi.org/10.1306/61EEDD14-173E-11D7-8645000102C1865D**

Wells, P.E., and Wells, G.M., 1994. Large-scale reorganization of ocean currents offshore Western Australia during the late Quaternary. *Marine Micropaleontology,* 24(2):157–186. **http://dx.doi.org/10.1016/0377-8398(94)90020-5**

Williams, M., Cook, E., van der Kaars, S., Barrows, T., Shulmeister, J., and Kershaw, P., 2009. Glacial and deglacial climatic patterns in Australia and surrounding regions from 35,000 to 10,000 years ago reconstructed from terrestrial and near-shore proxy data. *Quaternary Science Reviews,* 28(23–24):2398–2419. **http://dx.doi.org/10.1016/j.quascirev.2009.04.020**

Wyrwoll, K.-H., and Miller, G.H., 2001. Initiation of the Australian summer monsoon 14,000 years ago. *Quaternary International,* 83–85:119–128. **http://dx.doi.org/10.1016/S1040-6182(01)00034-9**

Wyrwoll, K.-H., Greenstein, B.J., Kendrick, G.W., and Chen, G.S., 2009. The palaeoceanography of the Leeuwin Current: implications for a future world. *Journal of the Royal Society of Western Australia,* 92(2):37–51. **http://www.rswa.org.au/publications/Journal/92(2)/ROY SOC 92.2 LEEUWIN 37-51.pdf**

Wyrwoll, K.-H., Hopwood, J.M., and Chen, G., 2012. Orbital time-scale circulation controls of the Australian summer monsoon: a possible role for mid-latitude Southern Hemisphere forcing? *Quaternary Science Reviews,* 35:23–28. **http://dx.doi.org/10.1016/j.quascirev.2012.01.003**

Wyrwoll, K.-H., Liu, Z., Chen, G., Kutzbach, J.E., and Liu, X., 2007. Sensitivity of the Australian summer monsoon to tilt and precession forcing. *Quaternary Science Reviews,* 26(25–28):3043–3057. **http://dx.doi.org/10.1016/j.quascirev.2007.06.026**

Xu, J., Kuhnt, W., Holbourn, A., Andersen, N., and Bartoli, G., 2006. Changes in the vertical profile of the Indonesian Throughflow during Termination II: evidence from the Timor Sea. *Paleoceanography,* 21(4):PA4202. **http://dx.doi.org/10.1029/2006PA001278**

Table T1. Expedition 356 primary and alternate site locations.

Site	Latitude	Longitude	Water depth (m)	Total penetration depth* (mbsf)	Adjacent industry well
Primary					
NWS-6A	28.6641°S	113.5778°E	152	330	Houtman-1
NWS-5A	27.3749°S	112.925°E	214	366	Morangie-1
NWS-4A	20.21438°S	115.06679°E	126	1055	West Tryal Rocks-2
NWS-3A	19.8223°S	115.7103°E	88	855	Fisher-1
NWS-2A	18.9653°S	117.6237°E	141	530	Picard-1
NWS-1A	18.3233°S	118.7337°E	146	370	Minilya-1
Alternate					
NWS-13A	28.671°S	113.5605°E	200	330	
NWS-12A	27.2802°S	112.8881°E	200	366	
NWS-11A	20.4736°S	114.8726°E	125	680†	
NWS-10A	20.5555°S	114.8777°E	200	1055	
NWS-9A	19.7978°S	115.7434°E	95	780	
NWS-8A	18.9122°S	117.5838°E	160	530	
NWS-7A	18.0652°S	118.6313°E	260	840	

* = Environmental Protection and Safety Panel (EPSP) approved, † = pending EPSP final approval. Adjacent industry wells are plugged and abandoned.

Table T2. Primary site operations and time estimates, Expedition 356.

Site	Location (latitude, longitude)	Seafloor depth (mbrf)	Operations description	Transit (days)	Drilling coring (days)	Wireline log (days)
Fremantle, Australia			**Begin expedition** 5.0	Port call days		
			Transit ~232 nmi @ 10.5 kt to NWS-6A	0.8		
NWS-6A	28.6641°S	163	Hole A - APC to 200 mbsf or refusal	0	0.9	0
EPSP	113.5778°E		Hole B - APC to 200 mbsf or refusal/XCB to 330 mbsf	0	1.3	0
330 mbsf			Hole C - APC to 200 mbsf or refusal/XCB to 330 mbsf, WL log	0	1.2	0.8
			Subtotal days on site: 4.3			
			Transit ~85 nmi @ 10.5 kt to NWS-5A	0.3		
NWS-5A	27.3749°S	225	Hole A - APC to 200 mbsf or refusal	0	0.7	0
EPSP	112.925°E		Hole B - APC to 200 mbsf or refusal/XCB to 346 mbsf	0	1.9	0
366 mbsf			Hole C - APC to 200 mbsf or refusal/XCB to 346 mbsf, WL log	0	1.8	0.9
			Subtotal days on site: 5.4			
			Transit ~469 nmi @ 10.5 kt to NWS-4A	1.9		
NWS-4A	20.21438°S	137	Hole A - APC to 200 mbsf or refusal	0	0.8	0
EPSP	115.06679°E		Hole B - APC to 200 mbsf or refusal then XCB to 600 mbsf or refusal	0	3.3	0
1055 mbsf			Hole C - APC to 200 mbsf or refusal then XCB to 600 mbsf or refusal	0	3.2	0
			Hole D - Drill to ~600 mbsf (XCB refusal), RCB to 1035 mbsf, WL log	0	6.1	2.2
			Subtotal days on site: 15.7			
			Transit ~43 nmi @ 10.5 kt to NWS-3A	0.2		
NWS-3A	19.8223°S	99	Hole A - APC to 200 mbsf or refusal	0	0.8	0
EPSP	115.7103°E		Hole B - APC to 200 mbsf or refusal then XCB to 600 mbsf or refusal	0	3.3	0
855 mbsf			Hole C - APC to 200 mbsf or refusal then XCB to 600 mbsf or refusal	0	2.8	0
			Hole D - Drill to ~600 mbsf (XCB depth), RCB to 835 mbsf, WL log	0	3.5	1.8
			Subtotal days on site: 12.3			
			Transit ~120 nmi @ 10.5 kt to NWS-2A	0.5		
NWS-2A	18.9653°S	152	Hole A - APC to 200 mbsf or refusal	0	0.8	0
EPSP	117.6237°E		Hole B - APC to 200 mbsf or refusal	0	2.1	0
530 mbsf			Hole C - APC to 200 mbsf or refusal then XCB to 510 mbsf, WL log	0	2.1	1.3
			Subtotal days on site: 6.3			
			Transit ~74 nmi @ 10.5 kt to NWS-1A	0.3		
NWS-1A	18.3233°S	157	Hole A - APC to 200 mbsf or refusal	0	0.8	0
EPSP	118.7337°E		Hole B - APC to 200 mbsf or refusal	0	1.6	0
370 mbsf			Hole C - APC to 200 mbsf or refusal then XCB to 350 mbsf, WL log	0	1.7	0.9
			Subtotal days on site: 5.0			
			Transit ~804 nmi @ 10.5 kt to Darwin	3.2		
Darwin, Australia			**End expedition** **Subtotals:**	**7.1**	**40.9**	**7.9**

Totals:
Port Call: 5.0
On-Site: 48.9
Operating Days: 56.0
Expedition: 61.0

Wireline logging includes triple combo, FMS-sonic, and VSI (25 m intervals). EPSP = Environmental Protection and Safety Panel. APC = advanced piston corer, XCB = extended core barrel, RCB = rotary core barrel, WL = wireline.

Table T3. Alternate site operations and time estimates, Expedition 356.

Site	Location (latitude, longitude)	Seafloor depth (mbrf)	Operations description	Drilling coring (days)	Wireline log (days)
NWS-13A EPSP 330 mbsf	28.671°S 113.5605°E	211	Hole A - APC to 200 mbsf or refusal Hole B - APC to 200 mbsf or refusal/XCB to 330 mbsf Hole C - APC to 200 mbsf or refusal/XCB to 330 mbsf, WL log **Subtotal days on site: 4.3**	0.9 1.3 1.2	0 0 0.8
NWS-12A EPSP 366 mbsf	27.2802°S 112.8881°E	211	Hole A - APC to 200 mbsf or refusal Hole B - APC to 200 mbsf or refusal/XCB to 346 mbsf Hole C - APC to 200 mbsf or refusal/XCB to 346 mbsf, WL log **Subtotal days on site: 5.4**	0.7 1.9 1.8	0 0 0.9
NWS-11A Pending EPSP 680 mbsf	20.4736°S 114.8726°E	136	Hole A - APC to 200 mbsf or refusal Hole B - APC to 200 mbsf or refusal then XCB to 600 mbsf or refusal Hole C - APC to 200 mbsf or refusal then XCB to 600 mbsf or refusal Hole D - Drill to ~600 mbsf (XCB depth), RCB to 660 mbsf, WL log **Subtotal days on site: 11.9**	0.8 3.3 2.7 3.3	0 0 0 1.8
NWS-10A EPSP 1055 mbsf	20.5555°S 114.8777°E	211	Hole A - APC to 200 mbsf or refusal Hole B - APC to 200 mbsf or refusal then XCB to 600 mbsf or refusal Hole C - APC to 200 mbsf or refusal then XCB to 600 mbsf or refusal Hole D - Drill to ~600 mbsf (XCB refusal), RCB to 1035 mbsf, WL log **Subtotal days on site: 15.7**	0.8 3.3 3.2 6.1	0 0 0 2.2
NWS-9A EPSP 780 mbsf	19.7978°S 115.7434°E	106	Hole A - APC to 200 mbsf or refusal Hole B - APC to 200 mbsf or refusal then XCB to 600 mbsf or refusal Hole C - APC to 200 mbsf or refusal then XCB to 600 mbsf or refusal Hole D - Drill to ~600 mbsf (XCB depth), RCB to 760 mbsf, WL log **Subtotal days on site: 12.3**	0.8 3.3 2.8 3.5	0 0 0 1.8
NWS-8A EPSP 530 mbsf	18.9122°S 117.5838°E	171	Hole A - APC to 200 mbsf or refusal Hole B - APC to 200 mbsf or refusal Hole C - APC to 200 mbsf or refusal then XCB to 510 mbsf, WL log **Subtotal days on site: 5.0**	0.8 1.6 1.7	0 0 0.9
NWS-7A EPSP 840 mbsf	18.0652°S 118.6313°E	271	Hole A - APC to 200 mbsf or refusal Hole B - APC to 200 mbsf or refusal then XCB to 600 mbsf or refusal Hole C - APC to 200 mbsf or refusal then XCB to 600 mbsf or refusal Hole D - Drill to ~600 mbsf (XCB depth), RCB to 820 mbsf, WL log **Subtotal days on site: 12.7**	0.8 3.4 2.9 3.7	0 0 0 1.8

Wireline logging includes triple combo, FMS-sonic, and VSI (25 m intervals). EPSP = Environmental Protection and Safety Panel. APC = advanced piston corer, XCB = extended core barrel, RCB = rotary core barrel, WL = wireline.

Figure F1. Map of the NWS showing major basins and location of modern and "fossil" reefs. Seismic data near Site NWS-4A is shown on Figure **F7.** Stars = primary and alternate sites, green circles = DSDP/ODP sites and other core locations referred to in text, yellow circles = industry well locations (Angel = Angel-1, G2/6/7 = Goodwyn-2, Goodwyn-6, Goodwyn-7, A1 = Austin-1, M/MN1 = Maitland/Maitland North-1, TR1 = West Tryal Rocks-1. WA = Western Australia, NT = Northern Territory, SA = South Australia, QLD = Queensland, NSW = New South Wales.

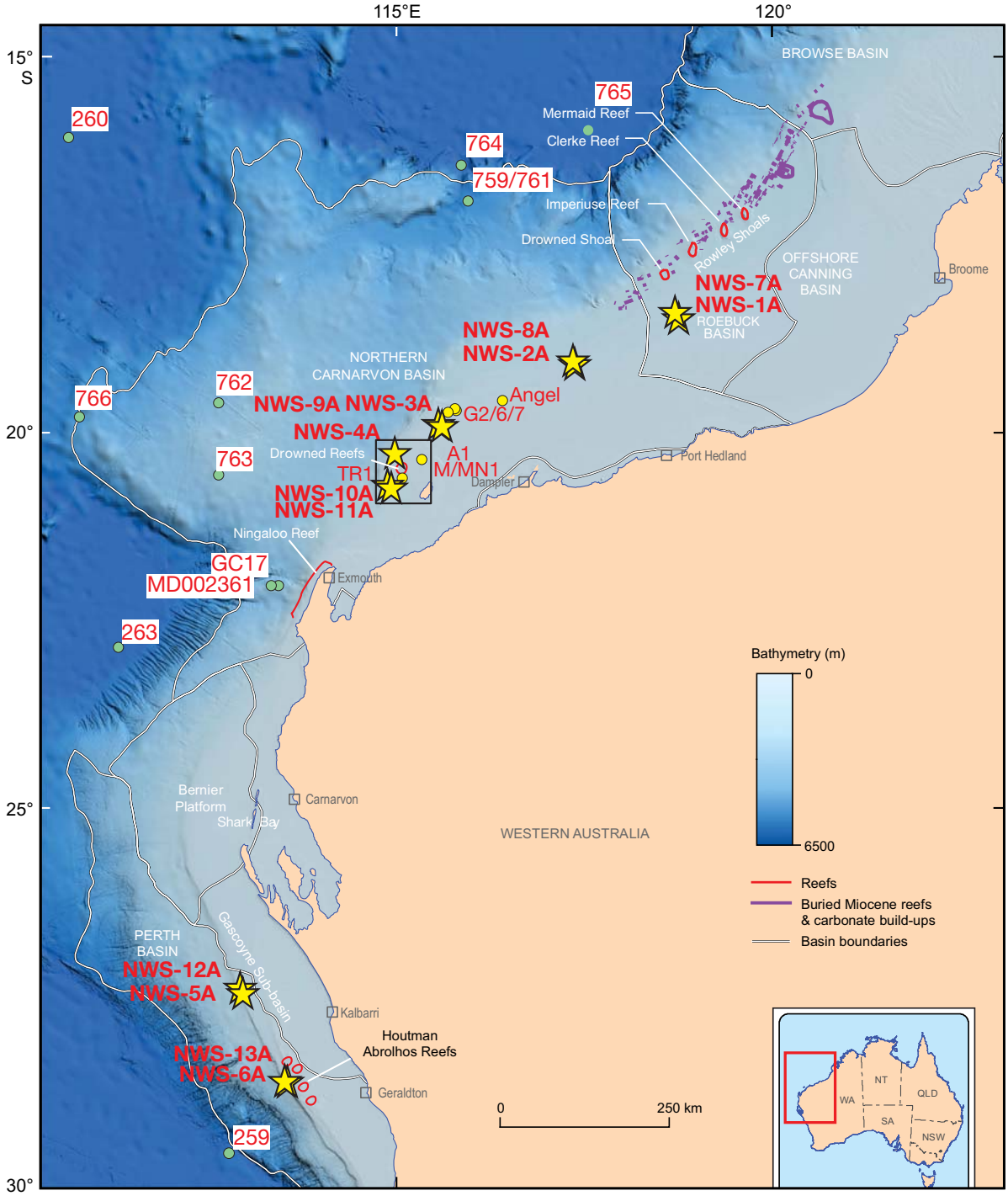

Figure F2. Oceanography and climate of the western Pacific (adapted from Gallagher et al., 2009). Currents (red = warm, blue = cold) are indicated. The direction (green arrows) and geographic extent of the summer monsoon (dashed green lines) are adapted from Kershaw et al. (2003). The average January position of the Intertropical Convergence Zone (ITCZ) is shown (cf. Huang et al., 2011). Yellow stars = position of the three groups of drilling sites: northern group (NWS-1A, NWS-2A, NWS-7A, and NWS-8A), second group (NWS-3A, NWS-4A, NWS-9A, NWS-10A, and NWS-11A), and most southerly group (NWS-5A, NWS-6A, NWS-12A, and NWS-13A).

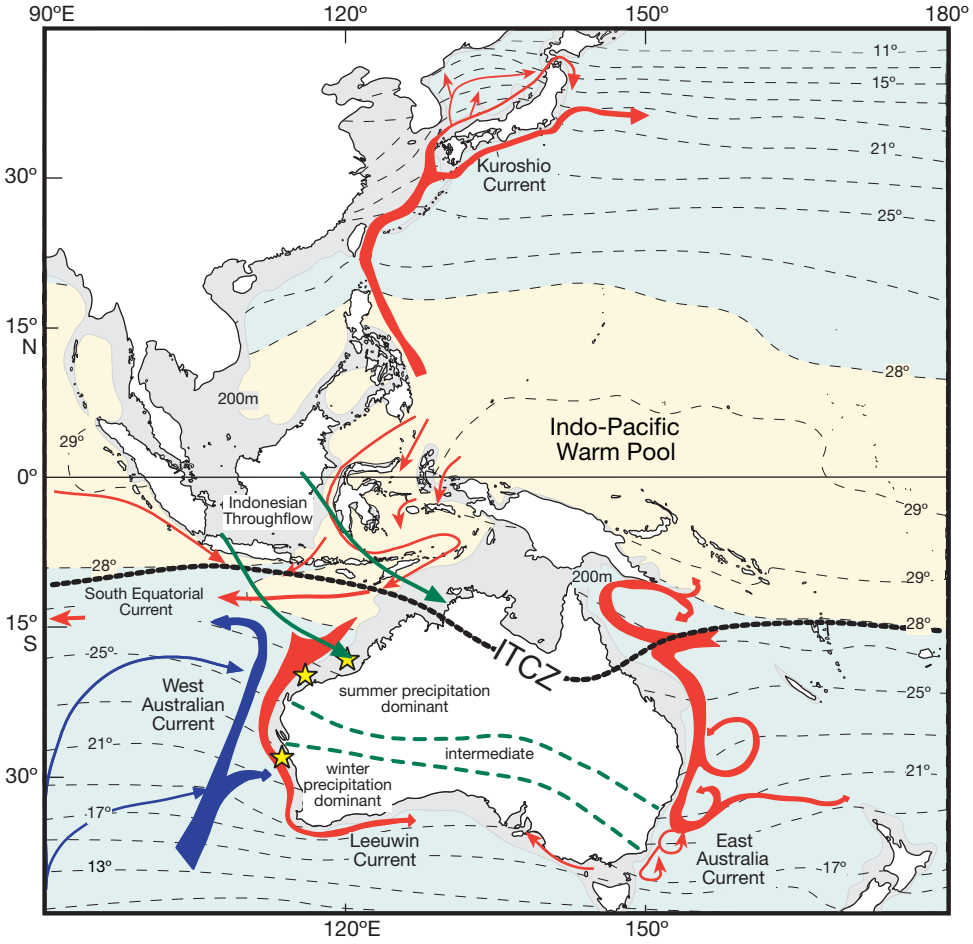

Figure F3. A. Benthic foraminifer $\delta^{18}O$ curve (LR2004) and MIS ages from Lisiecki and Raymo (2005) correlated with wells and cores in the Angel-1 region (see Fig. F1). **B.** Percent carbonate in Core BHC4. **C, F.** Oxygen isotopic data from three horizons in Core BHC4. Numerous individual foraminifers were analyzed at several horizons, and the average values for each calculated (A. Dutton, pers. comm., 2011). The values lie within the Quaternary ranges obtained from regional deep-sea studies (Wells and Wells, 1994). **D.** Percent carbonate in Core BHC1. **E.** Gamma log for Angel-1 (see Fig. F5). Vertical scale for B, C, D, and E is in meters and Cores BCH4, BCH1, and the Angel-1 well are ~50 m apart (Gallagher et al., in press).

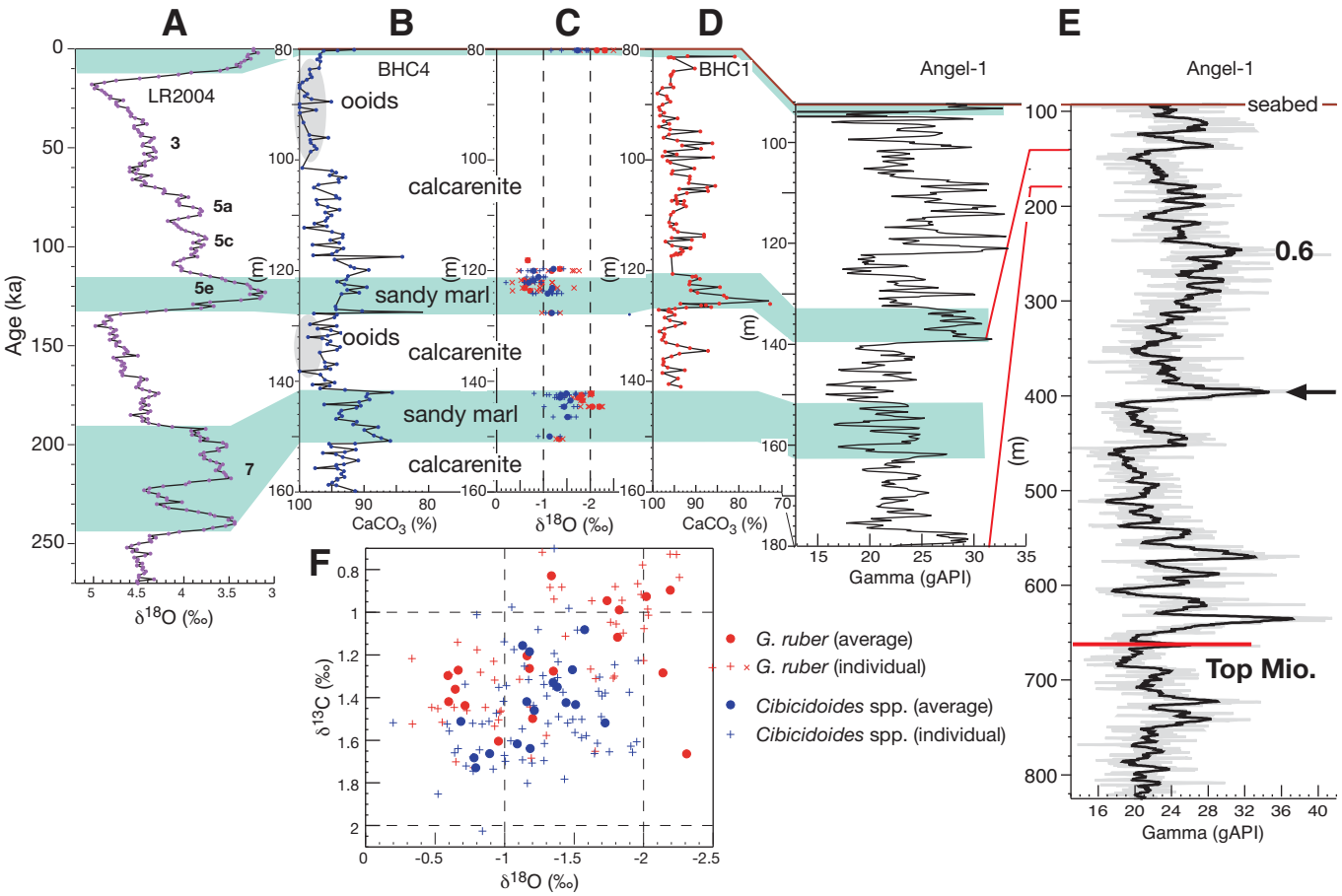

Figure F4. Pliocene–Pleistocene stratigraphy of the NWS and its relationship to various tectonic and climatic events. Horizontal shaded bars = likely periods of Indonesian seaway restriction. The benthic foraminifer $\delta^{18}O$ curve is from Lisiecki and Raymo (2005). The NWS Indo-Pacific foraminiferal species distribution (from cuttings) is from Gallagher et al. (2009) and preliminary unpublished results from the Fisher-1 well (adjacent to Site NWS-3A). Sea-surface temperature data are from Ocean Drilling Program (ODP) Hole 763A (Karas et al., 2011) (Fig. F1). ITF = Indonesian Throughflow.

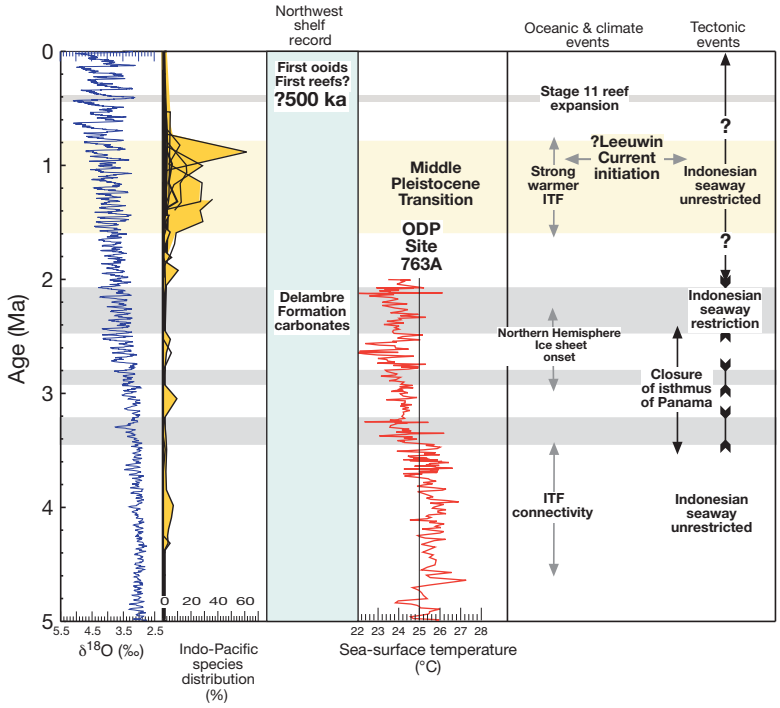

Figure F5. Correlation of gamma logs from eight wells (locations on Fig. F1) in the NWS (modified from Gallagher et al., in press). The vertical scale is in meters and the seabed is indicated. The top Miocene/base Pliocene (orange) is based on age data (green numbers) from Gallagher et al. (2009) for Goodwyn-7 and Goodwyn-6 and unpublished biostratigraphic data from sidewall cores in Fisher-1 well (adjacent to Site NWS-3A). The base of the Pliocene is poorly defined in Morangie-1 (adjacent to Site NWS-5A) and Houtman-1 (adjacent to Site NWS-6A) wells. However, well completion data suggest that it is ~500 meters below sea level. Additional stratigraphic data for Angel-1 well are shown in Figure F3. Black arrow = a possible correlation point in the Middle Pleistocene. The 0.6 (Ma) correlation datum is interpreted from stratigraphic data in Figure F6. The log data are corrected for borehole width effects. FM = formation.

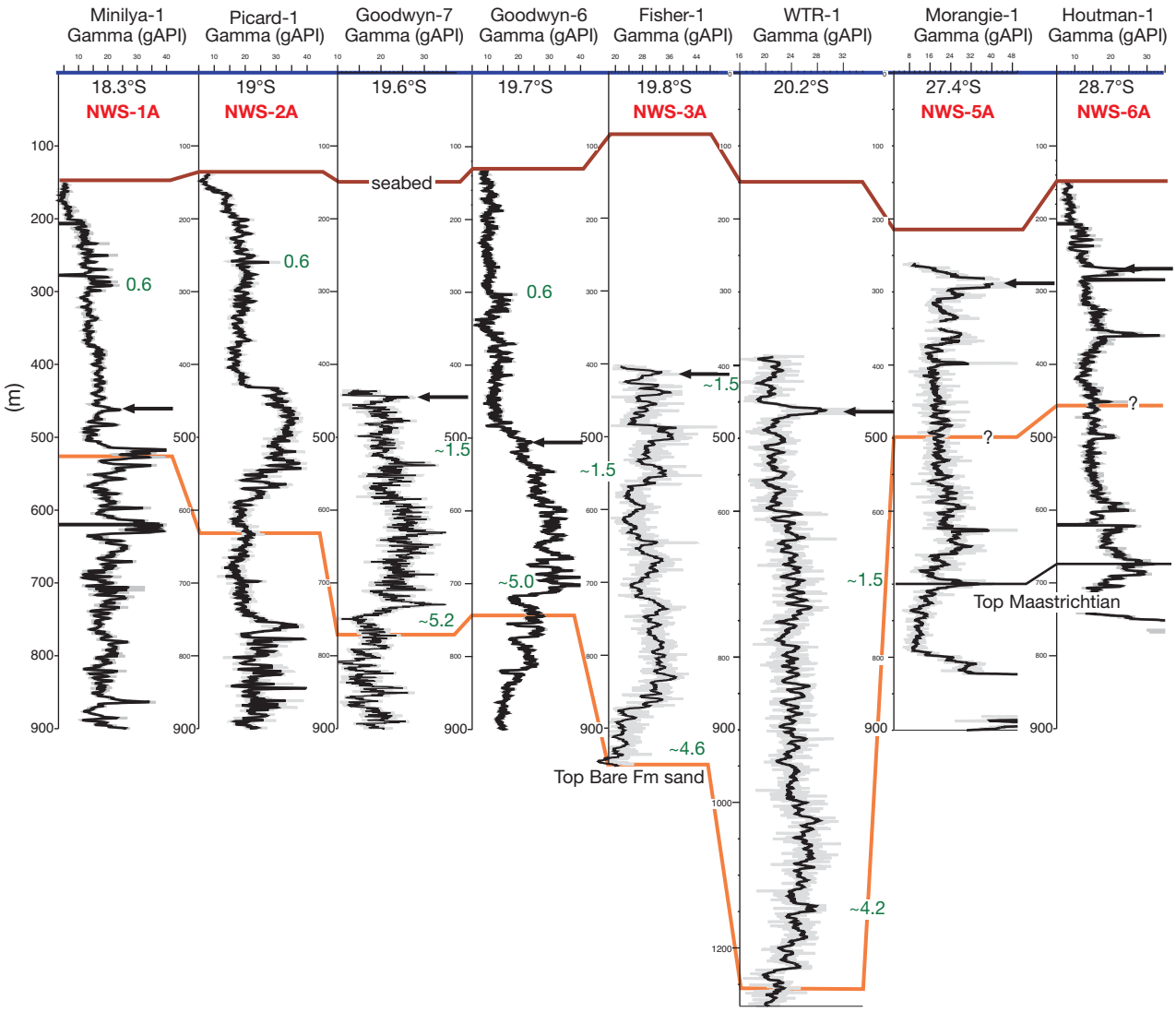

Figure F6. A, B. Gamma profiles (in depth) from Maitland North-1 and Austin-1 wells (Gallagher et al., 2009; in press). **C, D.** Gamma profiles of these two wells plotted with age. Intervals of increased clay input (gamma peaks) reflect relatively stronger monsoonal intensity. We also show the ages of known and predicted ooid occurrences and interpreted reef-building phases. **E.** Data from Maitland North-1 and Austin-1 wells are expanded to show possible correlations (0–1.0 Ma) to interglacial isotopic maxima in the LR2004 stack (Lisiecki and Raymo, 2005).

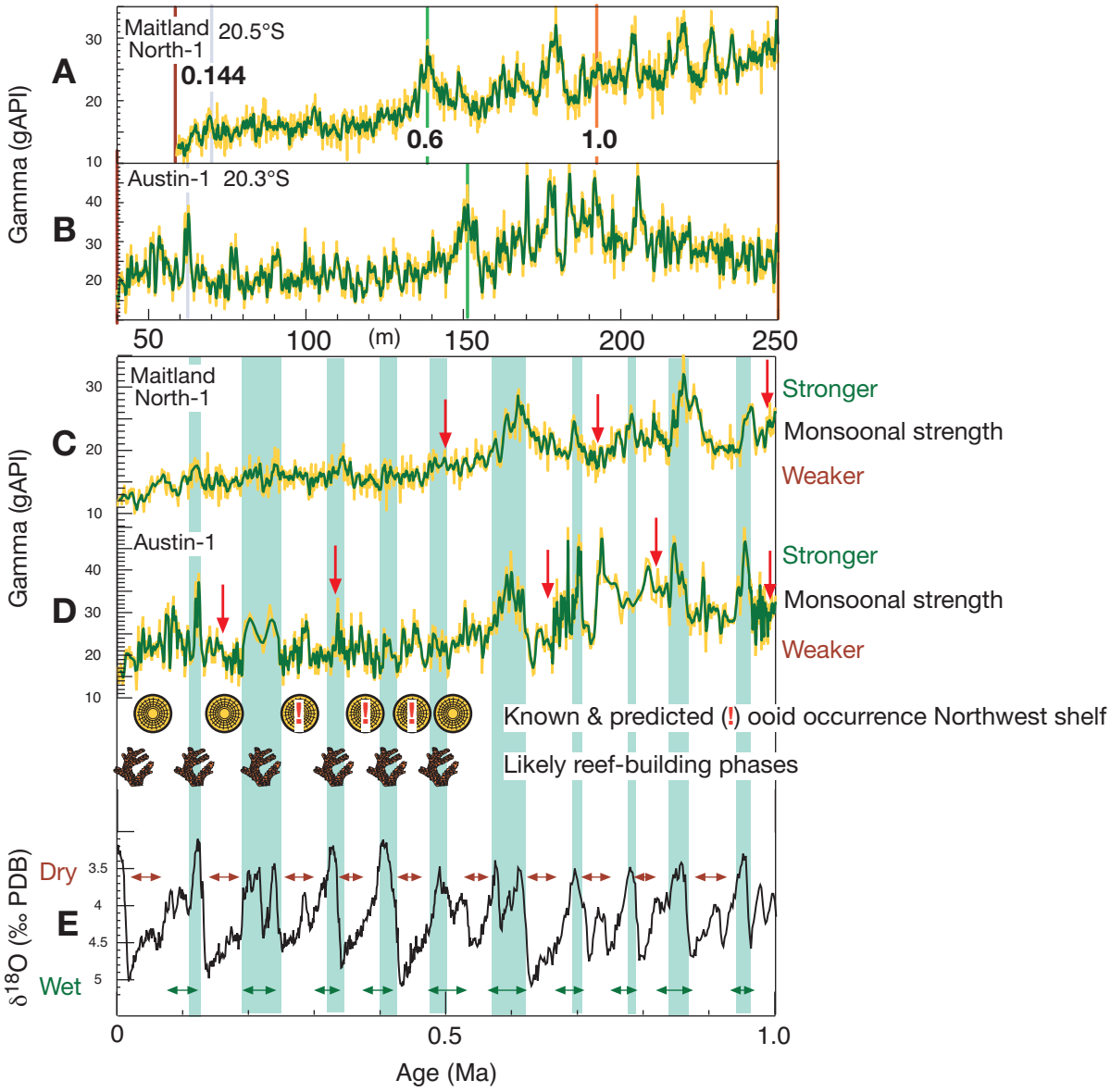

Figure F7. Primary Site NWS-4A (yellow star; adjacent industry well West Tryal Rocks-1 is also shown) on an interpreted seismic profile (A–A′) with "fossil" reefs (light green). See Gallagher et al. (2009) for age-depth model (from cuttings) for the five wells: West Tryal Rocks-1 (WTR 1), Tryal Rocks-1 (TR 1), Maitland North-1 (MN 1), Maitland-1 (M 1), and Austin-1 (A 1). The numbers (0.5–4.0) are reflector ages in millions of years. The section location is shown on Figure F1. FM = formation. Adapted from Gallagher et al. (in press).

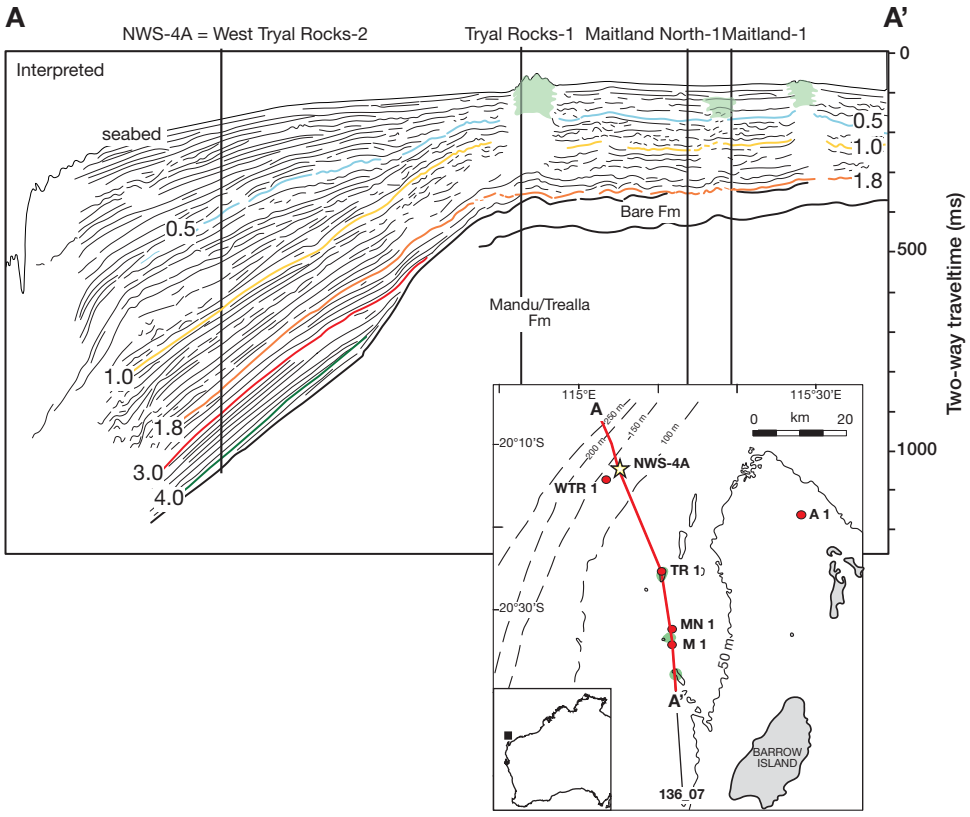

Figure F8. Plate tectonic history of the Australian plate for the last 70 m.y. Colors indicate the position of Australia in an absolute reference frame (Müller et al., 2008a) in 10 m.y. time steps from 70 Ma to present (filled gray Australia). Modified from Heine et al. (2010) with permission from Elsevier.

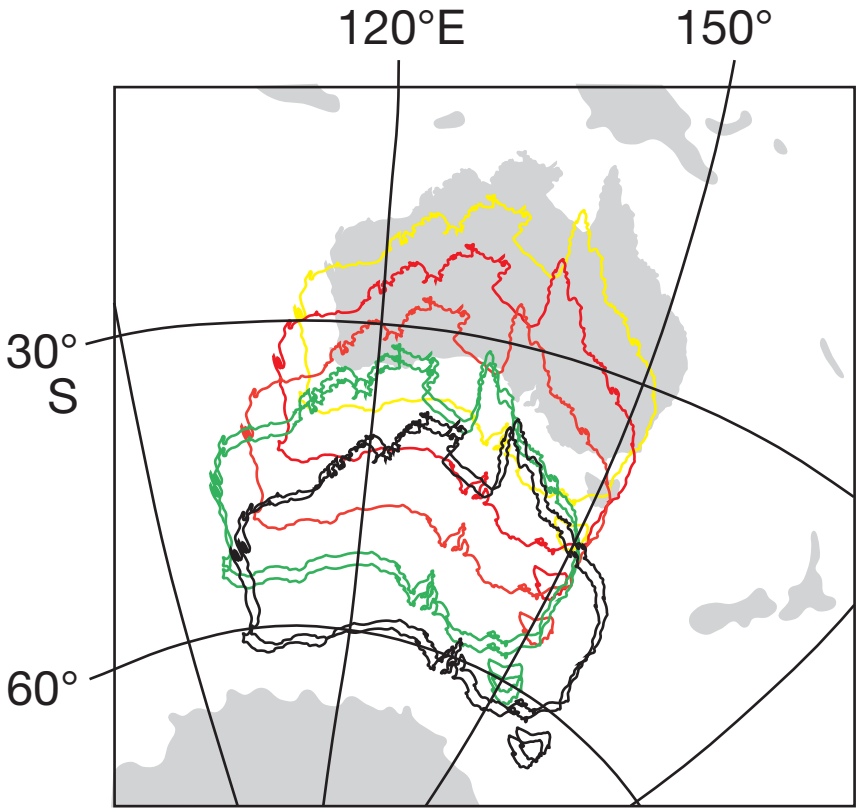

Figure F9. Global sea level (eustatic) curves and inundation history of the Australian continent based on paleoshorelines (Isern et al., 1995). Green curve = filtered global sea level curve (Haq and Al-Qahtani, 2005), black curve = global sea level curve (Haq et al., 1987), thick light blue line = filtered curve. Filtered lines show the long-wavelength component of the eustatic estimate using a cosine arch filter with a 10 m.y. window. Other curves include the Miller et al. (2005) and Kominz et al. (2008) sea level curves. All curves are plotted using the Gradstein et al. (2012) timescale. The amount of inundation is computed relative to the present-day 200 m isobath from the ETOPO2 global 2′ topography (NOAA, National Geophysical Data Center, 2006). Adapted from Heine et al. (2010).

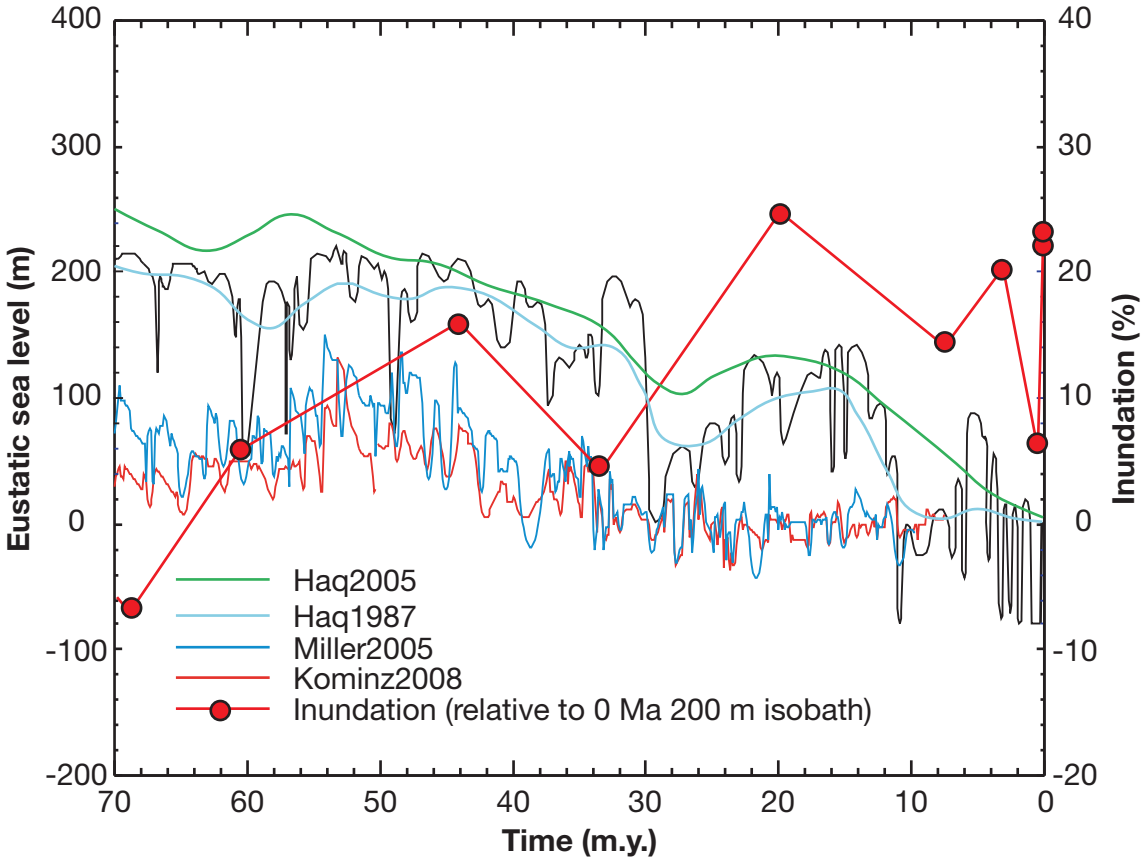

Site summaries

Site NWS-6A

Priority:	Primary
Position:	28.6641°S, 113.5778°E
Water depth (m):	152
Target drilling depth (mbsf):	330
Approved maximum penetration (mbsf):	330
Survey coverage (track map; seismic profile):	Map (Fig. **AF1**) Seismic profiles (Figs. **AF2, AF3**)
Objective(s):	This site is near the Houtman-Abrolhos main reef complex, which contains the most southerly tropical reefs in the Indian Ocean. Their evolution is directly related to the path of the Leeuwin Current. Dating, coupled with seismic correlation, may provide insight into the pre-Quaternary history of these reefs and a long-term perspective on Leeuwin Current evolution at the tropical/subtropical boundary off western Australia. It has been suggested that subsidence rates over 140 k.y. were very low compared to the reefs of the Carnarvon Basin (Collins and Testa, 2010). Subsidence analyses of the shelf wedge drilled at this site may extend this record back millions of years and allow more precise modeling of dynamic subsidence along the western margin of Australia. Finer grained facies in this section may also yield a Pliocene–Pleistocene record of the onset and variability of the southern Australian winter-dominated rainfall regime.
Drilling program:	Triple APC, double XCB
Logging program or downhole measurements program:	Triple combo, FMS, VSP
Nature of rock anticipated:	Calcarenites, calcilutites

Site summaries (continued)

Site NWS-5A

Priority:	Primary
Position:	27.3749°S, 112.9250°E
Water depth (m):	214
Target drilling depth (mbsf):	366
Approved maximum penetration (mbsf):	366
Survey coverage (track map; seismic profile):	Track map (Fig. **AF1**) Seismic profiles (Figs. **AF4, AF5**)
Objective(s):	This site, at the northern edge of the modern winter-dominated rainfall zone of southwestern Australia, is targeted to chart the timing of this regime; it is not likely to yield an orbital-scale climate record due to slope erosional processes. However, it will complement Site NWS-4A, as it is south of a climatic divide between the Australian monsoon–dominated north and the westerly wind-driven, winter rainfall–dominated south. It is also near the southern end of the north-south latitudinal transect and may provide a shelf to shelf-edge record of the tropical–subtropical transition related to Leeuwin Current activity. It is influenced by the anticlockwise, colder West Australian Current gyre, and the relative influence of this gyre versus the Leeuwin Current produces variations in paleoproductivity that may be documented over millions of years. Subsidence rates in this region are estimated to be significantly less than in the Carnarvon Basin further north because of variations in mantle dynamic subsidence between the Perth and Carnarvon Basins. Paleobathymetric analyses may produce the first detailed greater than million year subsidence record for this part of the West Australian margin, where previous subsidence estimates only extend to 125 ka.
Drilling program:	Triple APC, double XCB
Logging program or downhole measurements program:	Triple combo, FMS, VSP
Nature of rock anticipated:	Calcarenites, calcilutites

Site summaries (continued)

Site NWS-4A

Priority:	Primary
Position:	20.21438°S, 115.06679°E
Water depth (m):	126
Target drilling depth (mbsf):	1055
Approved maximum penetration (mbsf):	1055
Survey coverage (track map; seismic profile):	Track map (Fig. **AF6**) Seismic profile (Fig. **AF8**)
Objective(s):	The objective is to obtain an orbital-scale record of climate variability and monsoon history that may be comparable in its resolution to other global climate proxy records. In this shelf-margin setting, pollen is likely to be abundant, delivered by fluvial outflow during the rainy season. This site is also close to the southern edge of the Australian monsoon influence and can therefore be used chart its latitudinal variability. Marine microfossil paleoproductivity analyses may also reveal the dominance of the West Australian Current over the Leeuwin Current during glacial periods. The site lies downdip from a drowned reef on a paleoshelf edge. Therefore, by dating the reflectors and correlating them updip, it may be possible to constrain the reef onset age. Furthermore, downslope transported reefal or shelf detritus may enable analysis of reef and ramp development in response to variable sea level.
Drilling program:	Triple APC, double XCB followed by RCB to total depth
Logging program or downhole measurements program:	Triple combo, FMS, VSP
Nature of rock anticipated:	Calcilutites, calcarenites

Site summaries (continued)

Site NWS-3A

Priority:	Primary
Position:	19.8223°S, 115.7103°E
Water depth (m):	88
Target drilling depth (mbsf):	855
Approved maximum penetration (mbsf):	855
Survey coverage (track map; seismic profile):	Track map (Fig. **AF6**) Seismic profile (Fig. **AF9**)
Objective(s):	This site presents an opportunity to document the variation of ITF connectivity. It is also along strike from several drowned reefs. As a result, coring may allow the reflectors that pass beneath these reefs to be dated and therefore, by proxy, date reef onset. This site may also yield an interglacial Pliocene–Pleistocene record of the Australian monsoon and a detailed paleobathymetry and subsidence history.
Drilling program:	Triple APC, double XCB followed by RCB to total depth
Logging program or downhole measurements program:	Triple combo, FMS, VSP
Nature of rock anticipated:	Calcilutites, calcarenites

Site summaries (continued)

Site NWS-2A

Priority:	Primary
Position:	18.9653°S, 117.6237°E
Water depth (m):	141
Target drilling depth (mbsf):	530
Approved maximum penetration (mbsf):	530
Survey coverage (track map; seismic profile):	Track map (Fig. **AF11**) Seismic profile (Fig. **AF12**)
Objective(s):	The Pliocene–Pleistocene section may yield a tropical/subtropical carbonate record that may allow us to determine the subsidence, interglacial Australian monsoon, and tropical shelf edge oceanographic histories of the region. Oolitic facies may be present, and determining the age of these highly diagnostic tropical and paleodepth indices at this site may reveal their oldest occurrence in the Indian Ocean, enhancing our understanding of the onset of aridity in this region.
Drilling program:	Triple APC, double XCB
Logging program or downhole measurements program:	Triple combo, FMS, VSP
Nature of rock anticipated:	Calcilutites, calcarenites

Site summaries (continued)

Site NWS-1A

Priority:	Primary
Position:	18.3233°S, 118.7337°E
Water depth (m):	146
Target drilling depth (mbsf):	370
Approved maximum penetration (mbsf):	370
Survey coverage (track map; seismic profile):	Track map (Fig. **AF11**) Seismic profiles (Figs. **AF14, AF15**)
Objective(s):	This northernmost primary site will target the tropical to subtropical transition from the Pliocene to the Pleistocene updip from a drowned "fossil" reef. Improved ages for these reflectors will allow us to date this reef. The strata at this site may yield an interglacial record of the Australian monsoon. In addition, paleobathymetric analyses may shed light on the nature of the subsidence that drowned the nearby reef.
Drilling program:	Triple APC, double XCB
Logging program or downhole measurements program:	Triple combo, FMS, VSP
Nature of rock anticipated:	Calcilutites, calcarenites

Site summaries (continued)

Site NWS-13A

Priority:	Alternate
Position:	28.6710°S, 113.5605°E
Water depth (m):	200
Target drilling depth (mbsf):	330
Approved maximum penetration (mbsf):	330
Survey coverage (track map; seismic profile):	Track map (Fig. **AF1**) Seismic profile (Fig. **AF3**)
Objective(s):	This site is an alternate for Site NWS-6A. Dating, coupled with seismic correlation, may provide insights into the pre-Quaternary history of the reef complex and a long-term perspective on Leeuwin Current evolution at the tropical/subtropical boundary off western Australia. Subsidence analyses of the shelf wedge drilled may extend the record back millions of years and allow more precise modeling of dynamic subsidence along the western margin of Australia. Finer grained facies in this section may also yield a Pliocene–Pleistocene record of the onset and variability of the southern Australian winter-dominated rainfall regime.
Drilling program:	Triple APC, double XCB
Logging program or downhole measurements program:	Triple combo, FMS, VSP
Nature of rock anticipated:	Calcarenites, calcilutites

Site summaries (continued)

Site NWS-12A

Priority:	Alternate
Position:	27.2802°S, 112.8881°E
Water depth (m):	200
Target drilling depth (mbsf):	366
Approved maximum penetration (mbsf):	366
Survey coverage (track map; seismic profile):	Track map (Fig. **AF1**) Seismic profile (Fig. **AF5**)
Objective(s):	An alternate to Site NWS-5A, this site is located at the northern edge of the modern winter-dominated rainfall zone of southwestern Australia. It is south of a climatic divide between the Australian monsoon–dominated north and the westerly wind-driven, winter rainfall–dominated south. This site is near the southern end of the north-south latitudinal transect and may provide a shelf to shelf-edge record of the tropical–subtropical transition related to Leeuwin Current activity. It is also influenced by the anticlockwise, colder West Australian Current gyre and the relative influence of this gyre versus the Leeuwin Current produces variations in paleoproductivity that may be documented over millions of years. Subsidence rates in this region are estimated to be significantly less than in the Carnarvon Basin further north because of variations in mantle dynamic subsidence between the Perth and Carnarvon Basins. Paleobathymetric analyses may produce the first detailed greater than million year subsidence record for this part of the West Australian margin, where previous subsidence estimates only extend to 125 ka.
Drilling program:	Triple APC, double XCB
Logging program or downhole measurements program:	Triple combo, FMS, VSP
Nature of rock anticipated:	Calcarenites, calcilutites

Site summaries (continued)

Site NWS-11A

Priority:	Alternate
Position:	20.4736°S, 114.8726°E
Water depth (m):	125
Target drilling depth (mbsf):	680
Approved maximum penetration (mbsf):	Pending approval
Survey coverage (track map; seismic profile):	Track map (Fig. **AF6**) Seismic profile (Fig. **AF7**)
Objective(s):	This site is an alternate to Site NWS-4A. The primary objective is to obtain an orbital-scale record of climate variability and monsoon history comparable in its resolution to other global climate proxy records. Pollen is likely to be abundant, delivered by fluvial outflow during the rainy season. This location is also close to the southern edge of Australian monsoonal influence and can therefore be used to chart its latitudinal variability. Marine microfossil paleoproductivity analyses at this site may also reveal the dominance of the West Australian Current over the Leeuwin Current during glacial periods. The site is downdip from a tropical ramp and directly underneath the path of the Leeuwin Current. Therefore, the section may also be used to chart tropical oceanographic variability on an orbital scale. This site is pending final EPSP approval.
Drilling program:	Triple APC, double XCB, RCB if necessary
Logging program or downhole measurements program:	Triple combo, FMS, VSP
Nature of rock anticipated:	Calcilutites, calcarenites

Site summaries (continued)

Site NWS-10A

Priority:	Alternate
Position:	20.5555°S, 114.8777°E
Water depth (m):	200
Target drilling depth (mbsf):	1055
Approved maximum penetration (mbsf):	1055
Survey coverage (track map; seismic profile):	Track map (Fig. **AF6**) Seismic profile (Fig. **AF7**)
Objective(s):	This site is an alternate to Site NWS-4A. The primary objective is to obtain an orbital-scale record of climate variability and monsoon history comparable in its resolution to other global climate proxy records. Pollen is likely to be abundant, delivered by fluvial outflow during the rainy season. This location is also close to the southern edge of Australian monsoonal influence and can therefore be used to chart its latitudinal variability. Marine microfossil paleoproductivity analyses may also reveal the dominance of the West Australian Current over the Leeuwin Current during glacial periods. The site is downdip from a tropical ramp and directly underneath the path of the Leeuwin Current. Therefore, the section may also be used to chart tropical oceanographic variability on an orbital scale.
Drilling program:	Triple APC, double XCB followed by RCB to total depth
Logging program or downhole measurements program:	Triple combo, FMS, VSP
Nature of rock anticipated:	Calcilutites, calcarenites

Site summaries (continued)

Site NWS-9A

Priority:	Alternate
Position:	19.7978°S, 115.7434°E
Water depth (m):	95
Target drilling depth (mbsf):	780
Approved maximum penetration (mbsf):	780
Survey coverage (track map; seismic profile):	Track map (Fig. **AF6**) Seismic profiles (Figs. **AF9, AF10**)
Objective(s):	This site is an alternate to Site NWS-3A. This site presents an opportunity to document the variation of ITF connectivity. It is also along strike from several drowned reefs. As a result, coring may allow the reflectors that pass beneath these reefs to be dated and therefore, by proxy, date reef onset. This site may also yield an interglacial Pliocene–Pleistocene record of the Australian monsoon and a detailed paleobathymetry and subsidence history.
Drilling program:	Triple APC, double XCB followed by RCB to total depth
Logging program or downhole measurements program:	Triple combo, FMS, VSP
Nature of rock anticipated:	Calcilutites, calcarenites

Site summaries (continued)

Site NWS-8A

Priority:	Alternate
Position:	18.9122°S, 117.5838°E
Water depth (m):	160
Target drilling depth (mbsf):	530
Approved maximum penetration (mbsf):	530
Survey coverage (track map; seismic profile):	Track map (Fig. **AF11**) Seismic profiles (Figs. **AF12, AF13**)
Objective(s):	This site is an alternate to Site NWS-2A. The Pliocene–Pleistocene section may yield a tropical/subtropical carbonate record to help determine the subsidence, interglacial Australian Monsoon, and tropical shelf edge oceanographic histories of the region. Oolitic facies may be present in this section, and determining the age of these highly diagnostic tropical and paleodepth indices may reveal their oldest occurrence in the Indian Ocean, enhancing our understanding of the onset of aridity in this region.
Drilling program:	Triple APC, double XCB
Logging program or downhole measurements program:	Triple combo, FMS, VSP
Nature of rock anticipated:	Calcilutites, calcarenites

Site summaries (continued)

Site NWS-7A

Priority:	Alternate
Position:	18.0652°S, 118.6313°E
Water depth (m):	260
Target drilling depth (mbsf):	840
Approved maximum penetration (mbsf):	840
Survey coverage (track map; seismic profile):	Track map (Fig. **AF11**) Seismic profile (Fig. **AF15**)
Objective(s):	An alternate to Site NWS-1A, this northernmost site targets the tropical to subtropical transition from the Pliocene to the Pleistocene updip from a drowned fossil reef. Improved ages for these reflectors will allow us to date this reef. The strata at this site may yield an interglacial record of the Australian monsoon. In addition, paleobathymetric analyses may shed light on the nature of the subsidence that drowned the nearby reef.
Drilling program:	Triple APC, double XCB followed by RCB to total depth
Logging program or downhole measurements program:	Triple combo, FMS, VSP
Nature of rock anticipated:	Calcilutites, calcarenites

Figure AF1. Bathymetric map showing the seafloor around primary Sites NWS-6A and NWS-5A and alternate Sites NWS-13A and NWS-12A. Bathymetric data are derived from the Geoscience Australia Australian bathymetry and topography grid, June 2009. The positions of multichannel seismic profiles are shown. The Houtman Abrolhos reef complex is the most southerly reef system in the Indian Ocean.

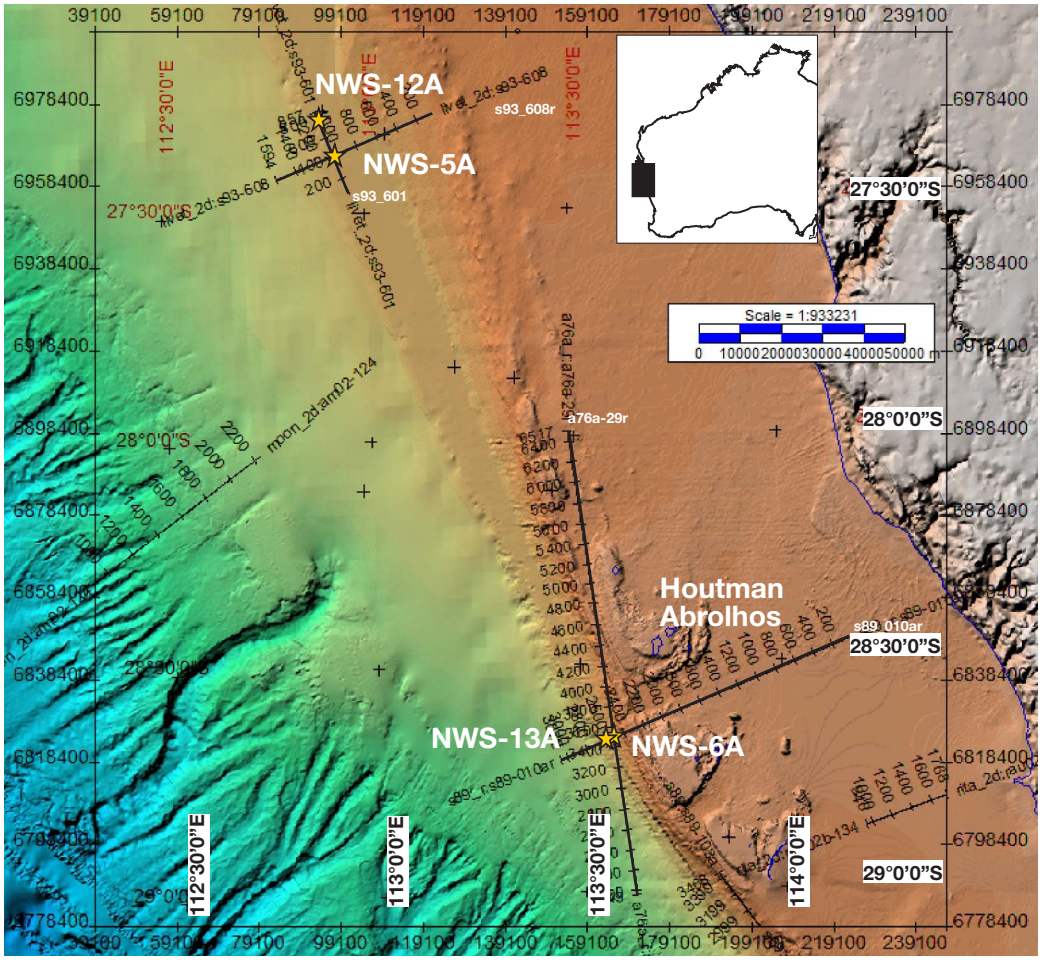

Figure AF2. Multichannel seismic profile across primary Site NWS-6A. Green line = inferred base of the Pliocene–Pleistocene. TWT = two-way traveltime.

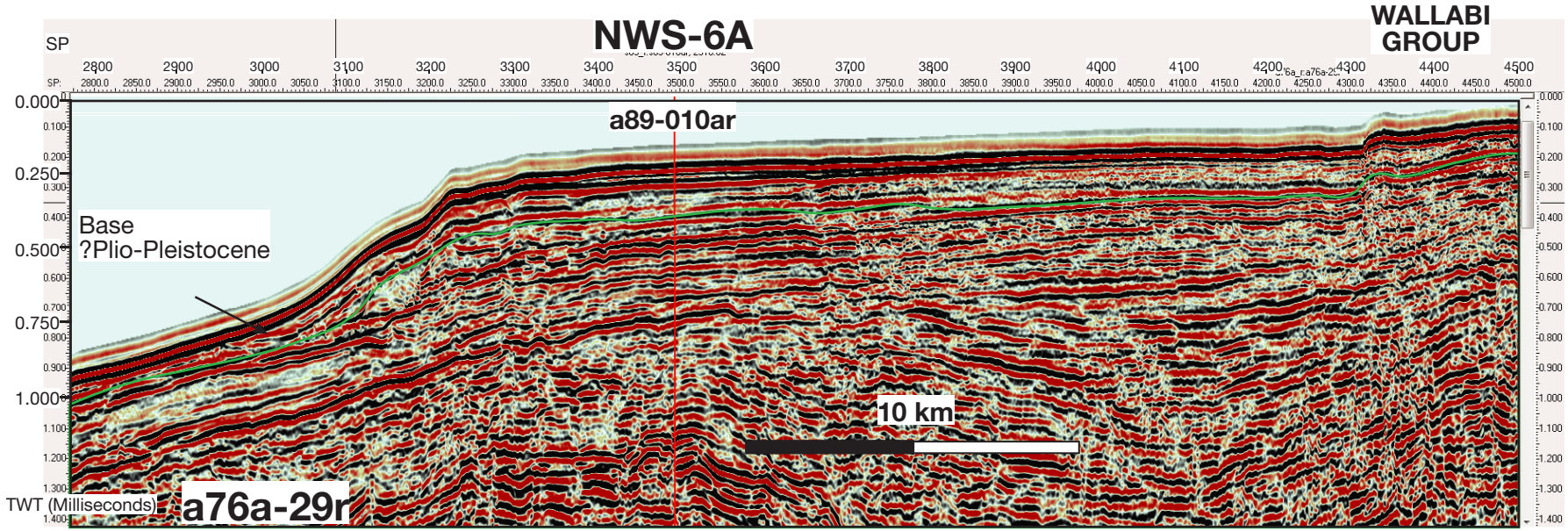

Figure AF3. Multichannel seismic profile across primary Site NWS-6A and alternate Site NWS-13A. The top of the green shaded area indicates the inferred base of the Pliocene–Pleistocene. TWT = two-way traveltime. Question marks (????) indicate the exact location of the base of the Pliocene boundary is not known.

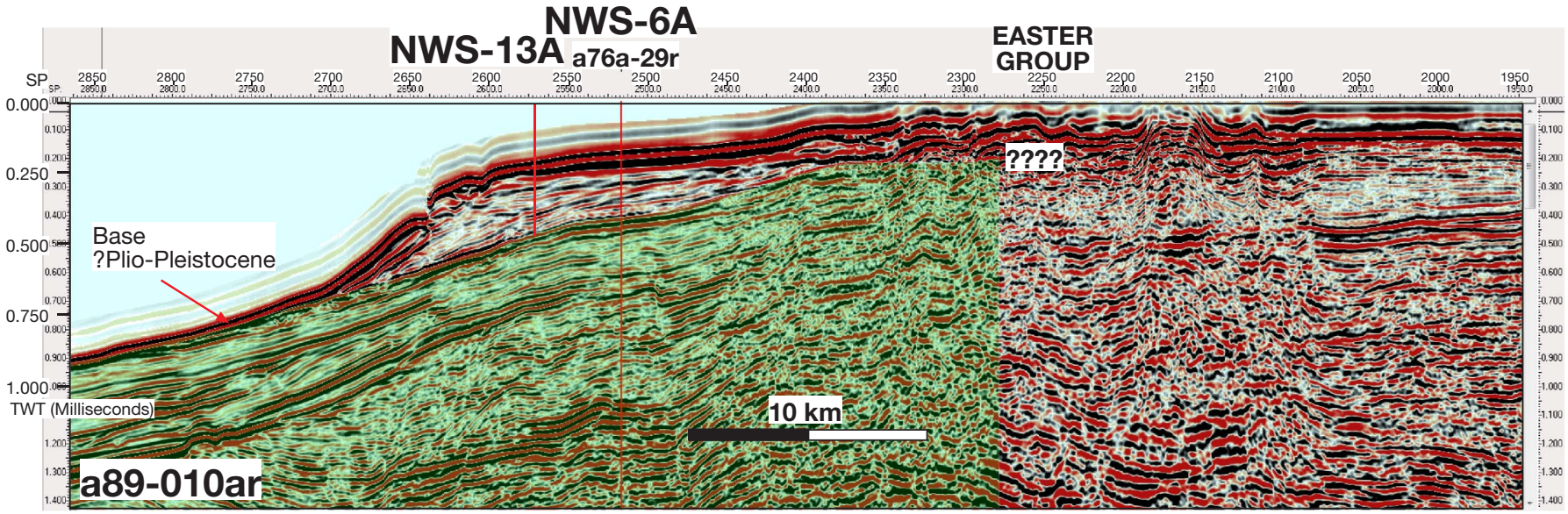

Figure AF4. Multichannel seismic profile across primary Site NWS-5A. The inferred base of the Pliocene–Pleistocene is at the top of the green shaded section. TWT = two-way traveltime.

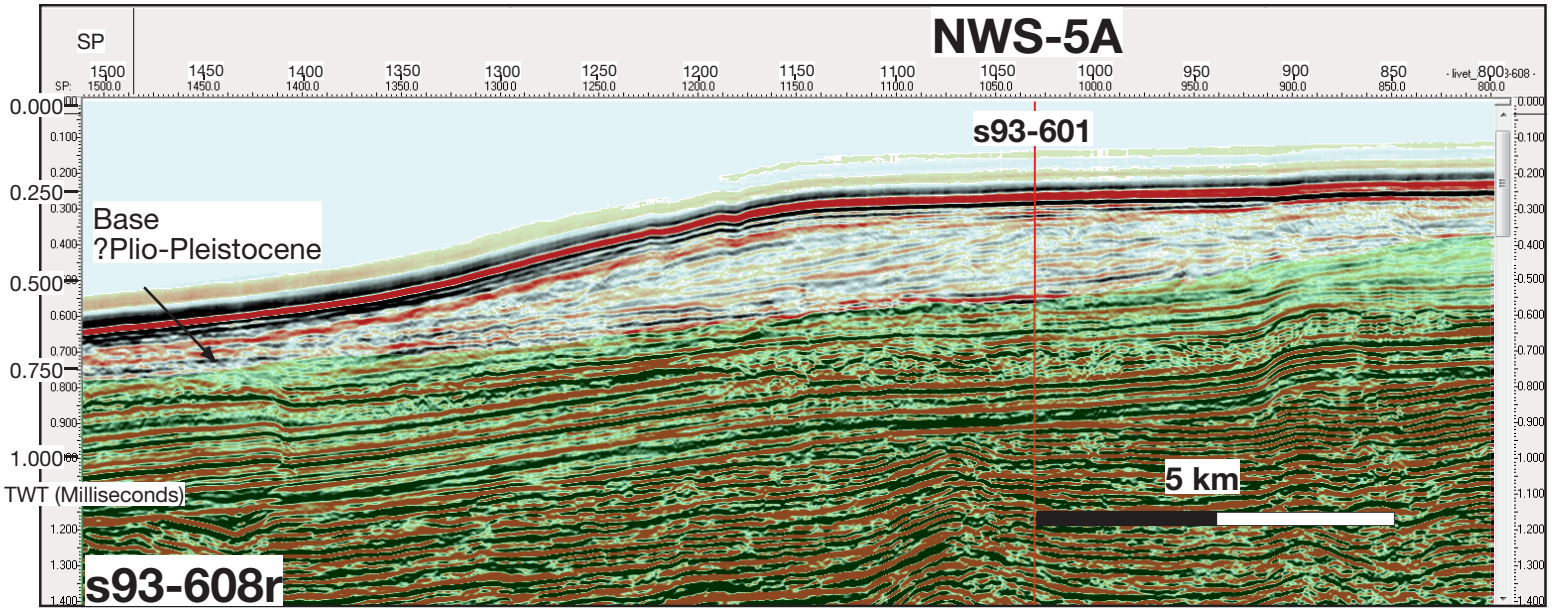

Figure AF5. Multichannel seismic profile across primary Site NWS-5A and alternate Site NWS-12A. The inferred base of the Pliocene–Pleistocene is at the top of the green shaded section. TWT = two-way traveltime.

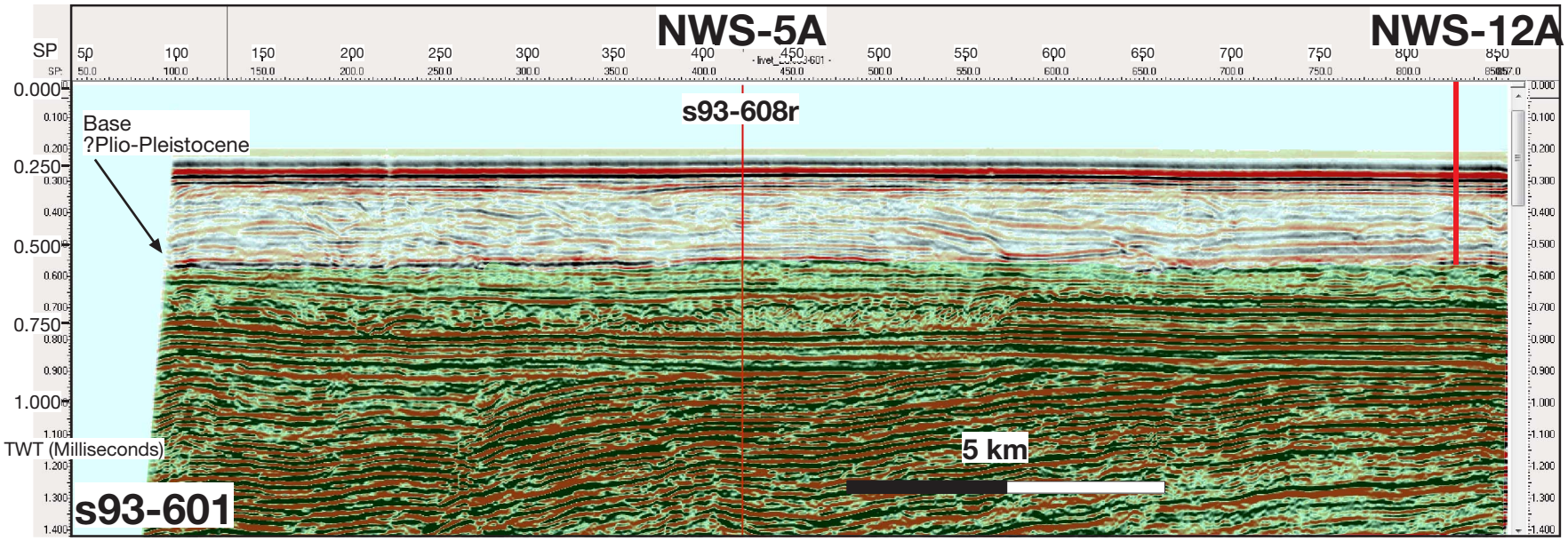

Figure AF6. Bathymetric map showing the seafloor around primary Sites NWS-3A and NWS-4A and alternate Sites NWS-9A, NWS-10A and NWS-11A. Bathymetric data are derived from the Geoscience Australia Australian bathymetry and topography grid, June 2009. The positions of multichannel seismic profiles are shown. Green lines indicate positions of gas pipelines.

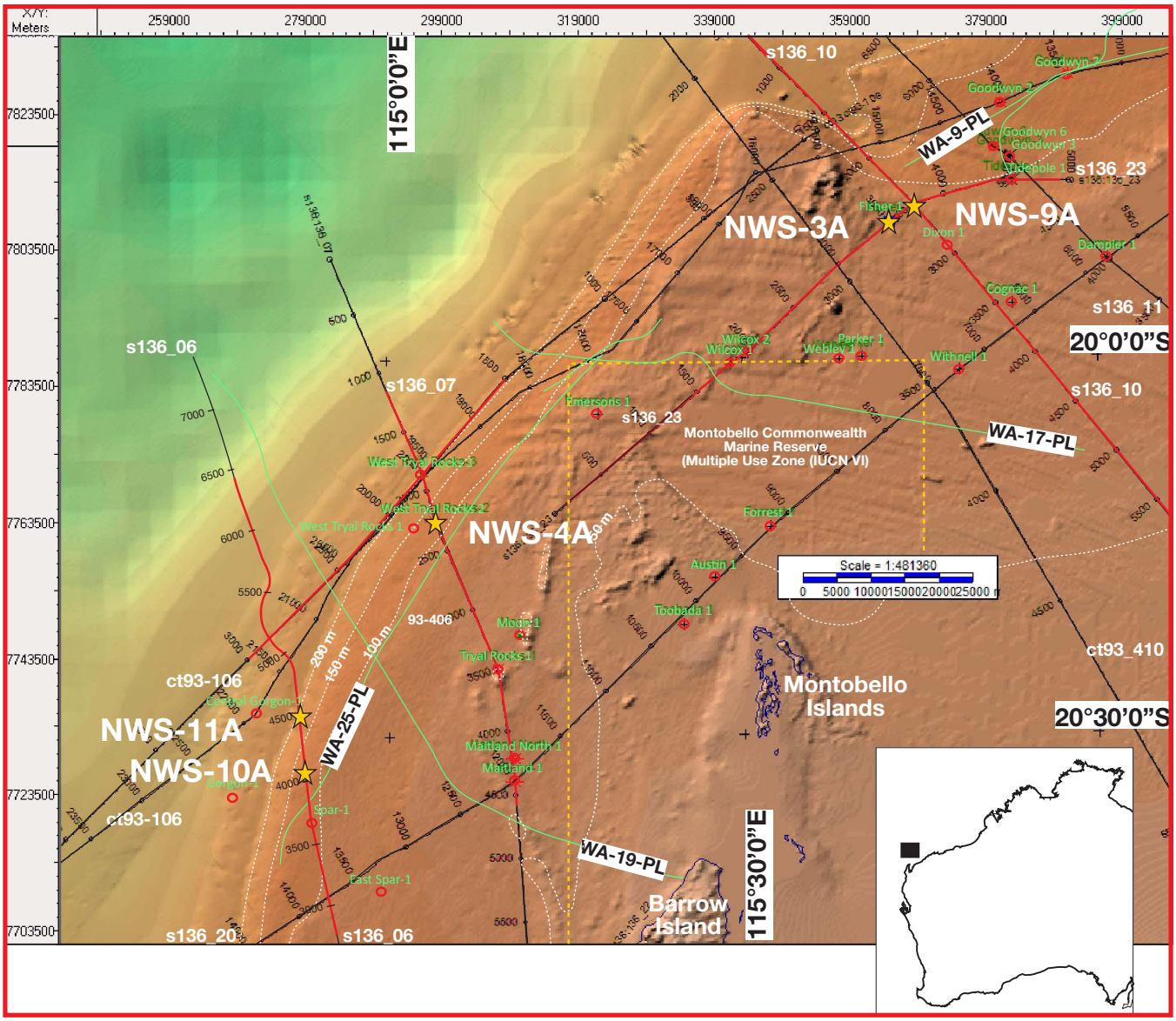

Figure AF7. Multichannel seismic profile across alternate Sites NWS-10A and NWS-11A. TWT = two-way traveltime.

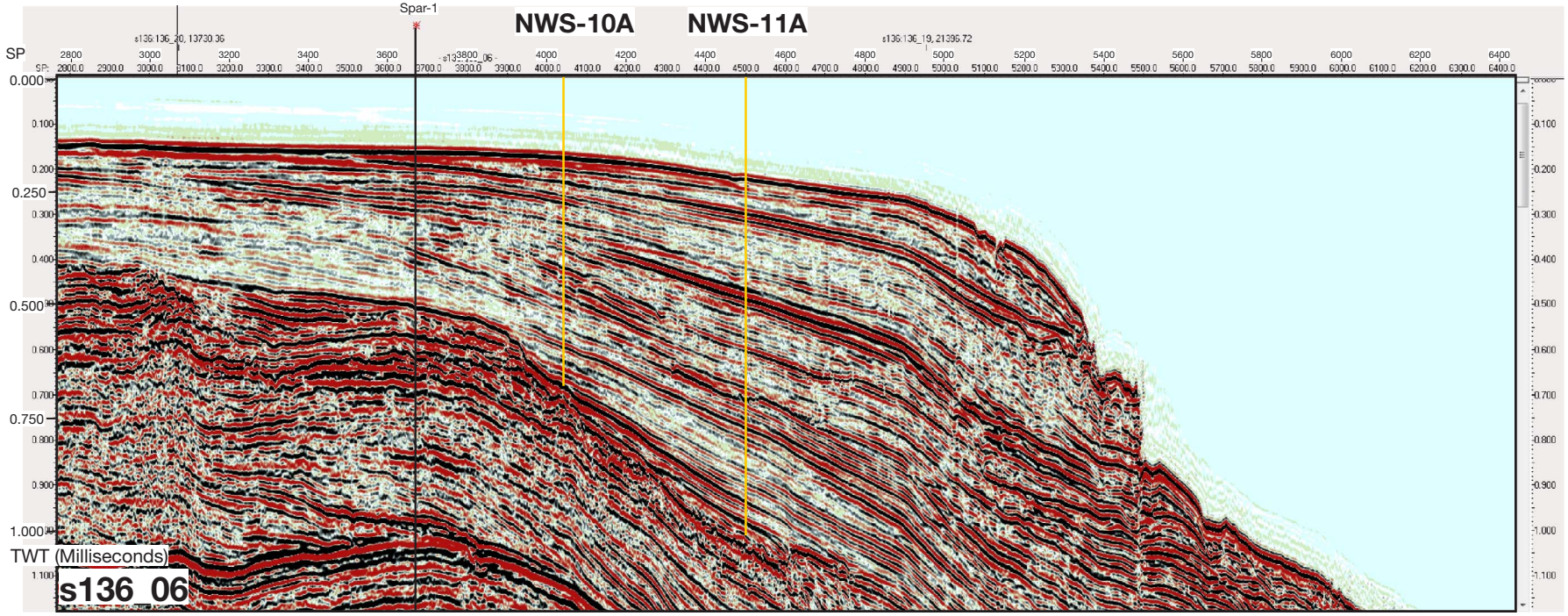

Figure AF8. Multichannel seismic profile across primary Site NWS-4A. Green line denotes the inferred top of the Miocene. TWT = two-way traveltime. FM = formation.

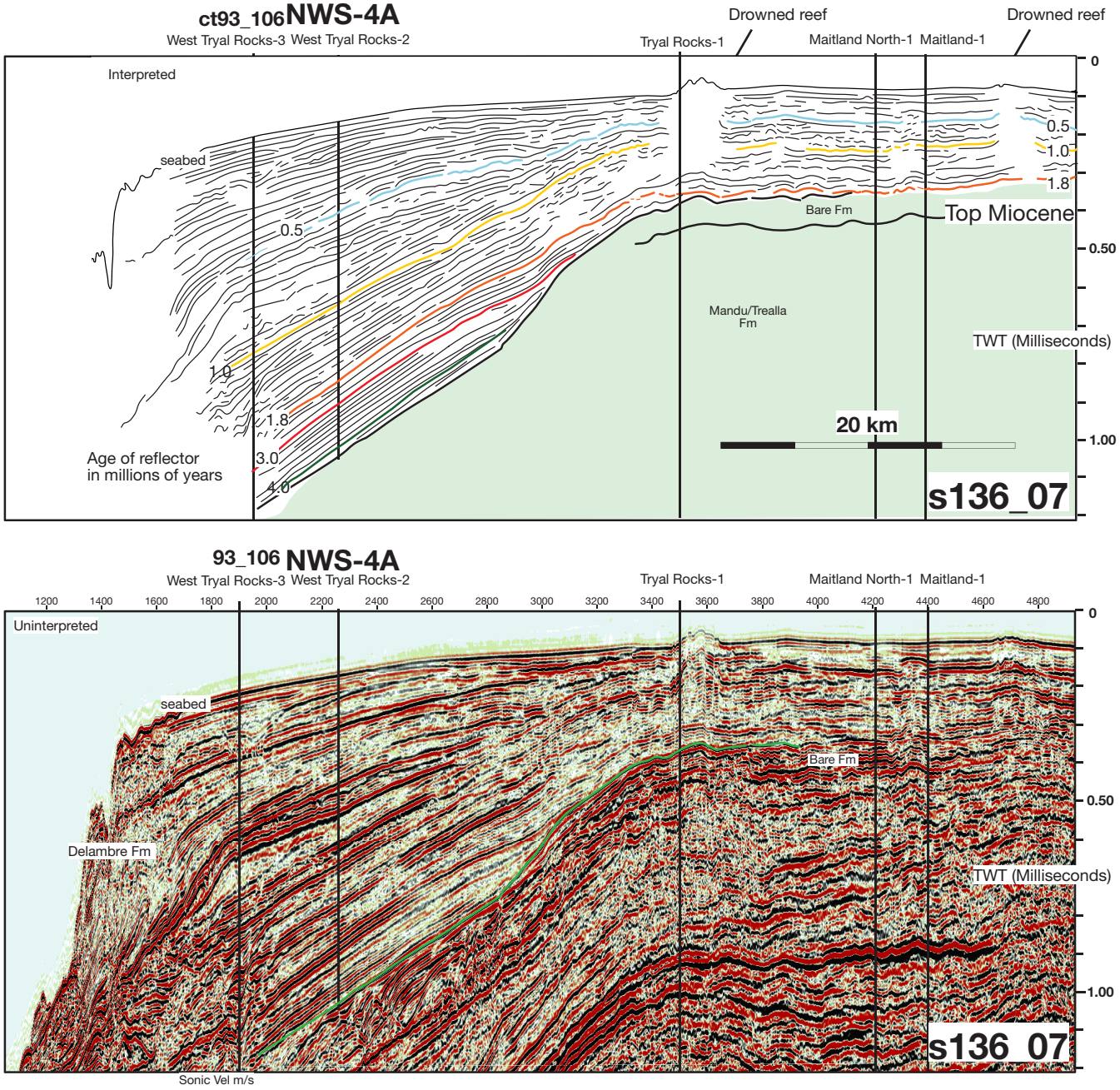

Figure AF9. Multichannel seismic profile across primary Site NWS-3A and alternate Site NWS-9A. Green line denotes the inferred top of the Miocene. TWT = two-way traveltime.

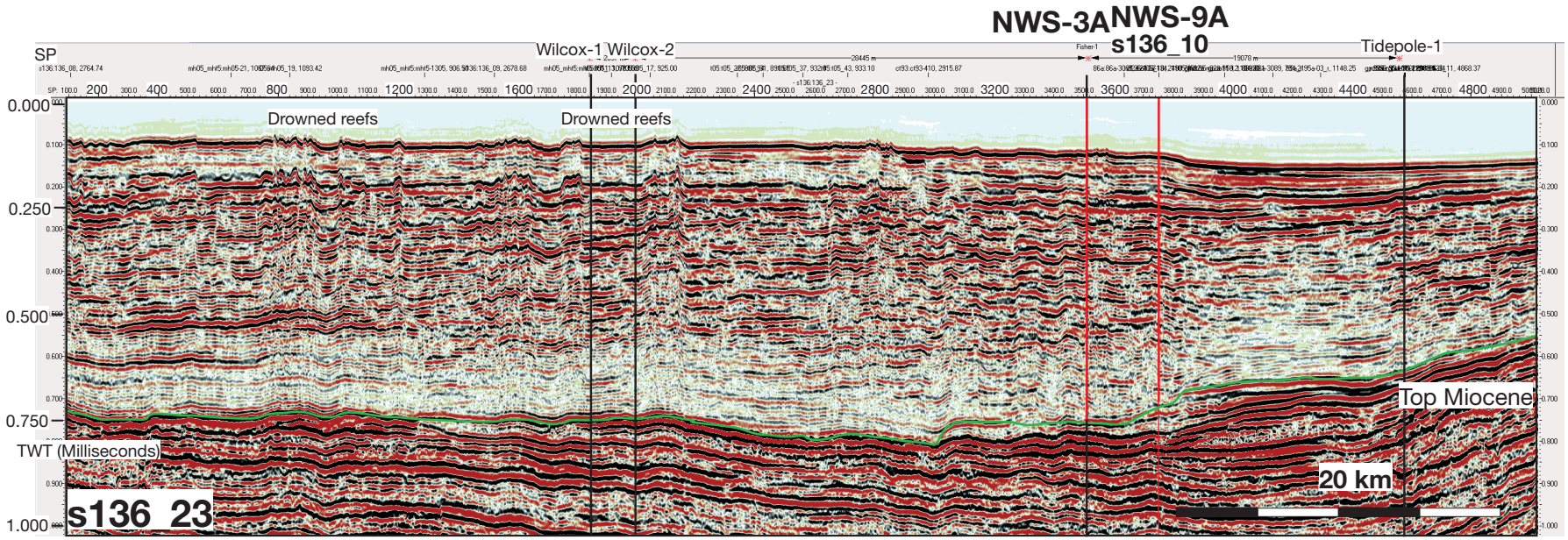

Figure AF10. Multichannel seismic profile across alternate Site NWS-9A. The top of the green shaded section is the inferred top of the Miocene. TWT = two-way traveltime.

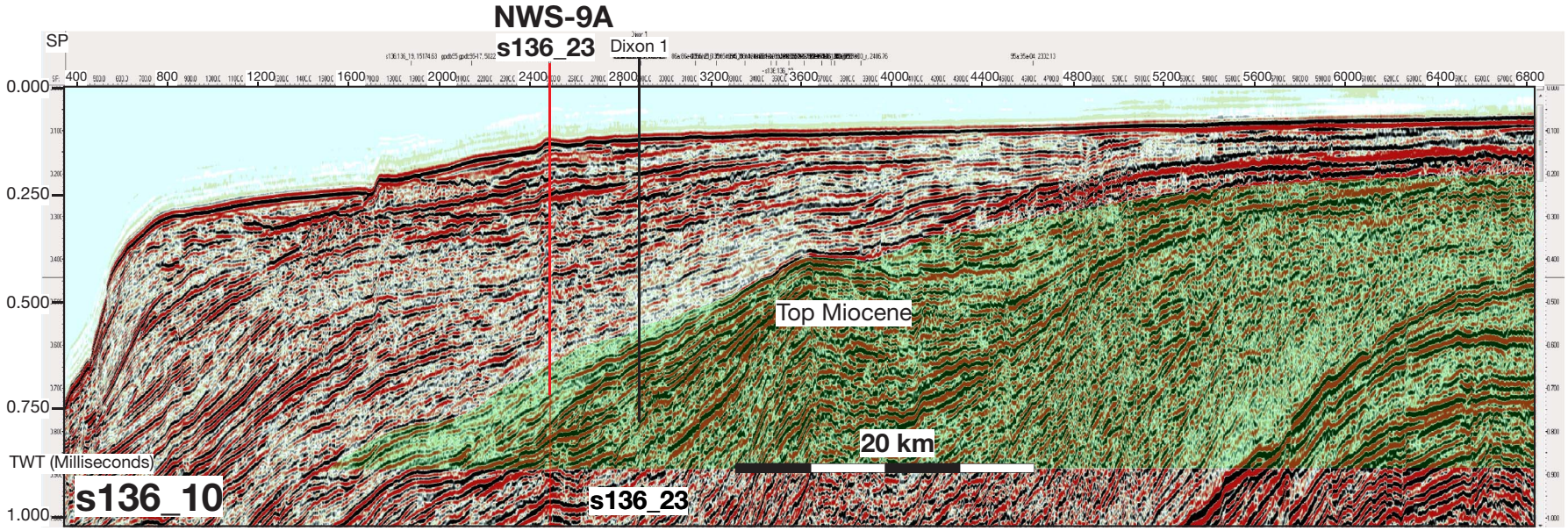

Figure AF11. Bathymetric map showing the seafloor around primary Sites NWS-1A and NWS-2A and alternate Sites NWS-7A and NWS-8A. Bathymetric data are derived from the Geoscience Australia Australian bathymetry and topography grid, June 2009. The positions of multichannel seismic profiles are shown. The Rowley Shoals are a series of three atolls close to the seismic profiles.

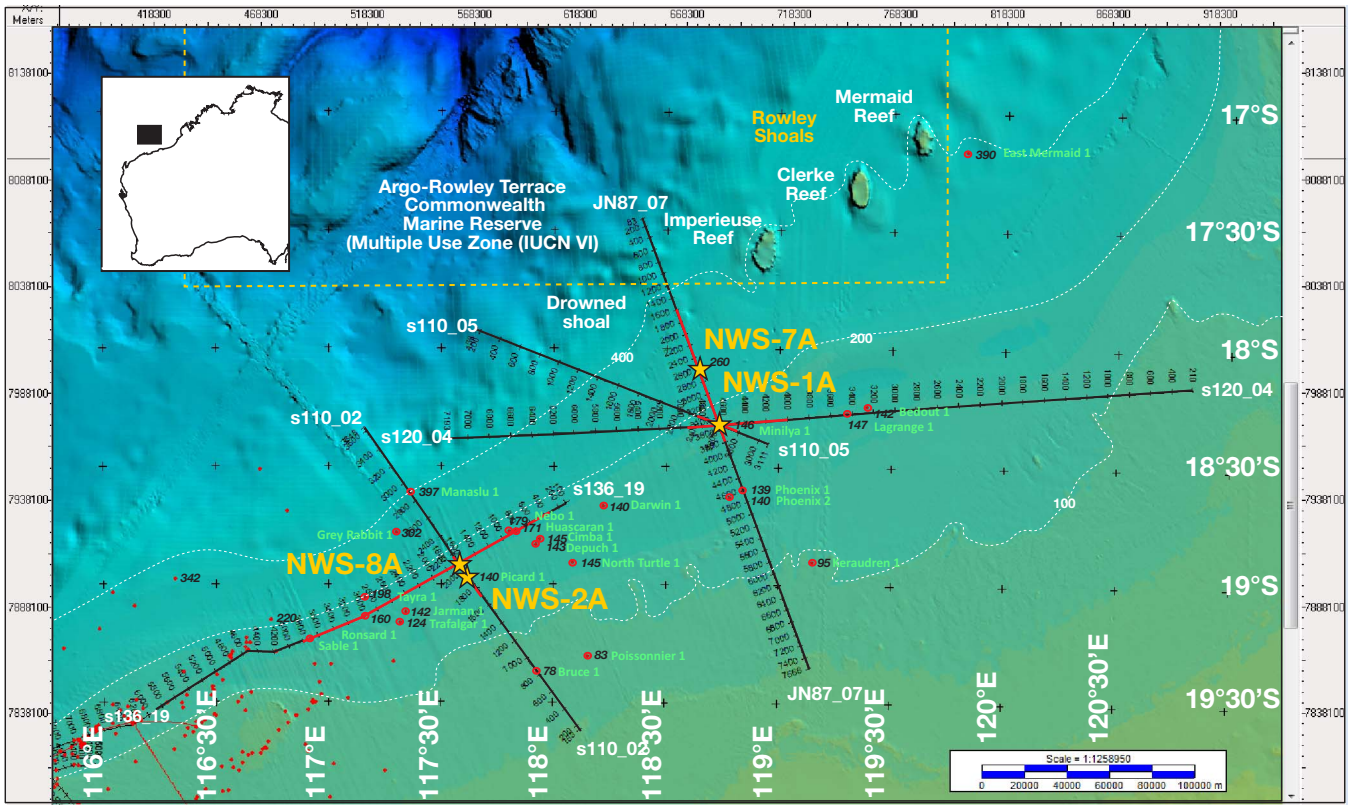

Figure AF12. Multichannel seismic profile across primary Site NWS-2A and alternate Site NWS-8A. The top of the green shaded section is the inferred top of the Miocene. TWT = two-way traveltime.

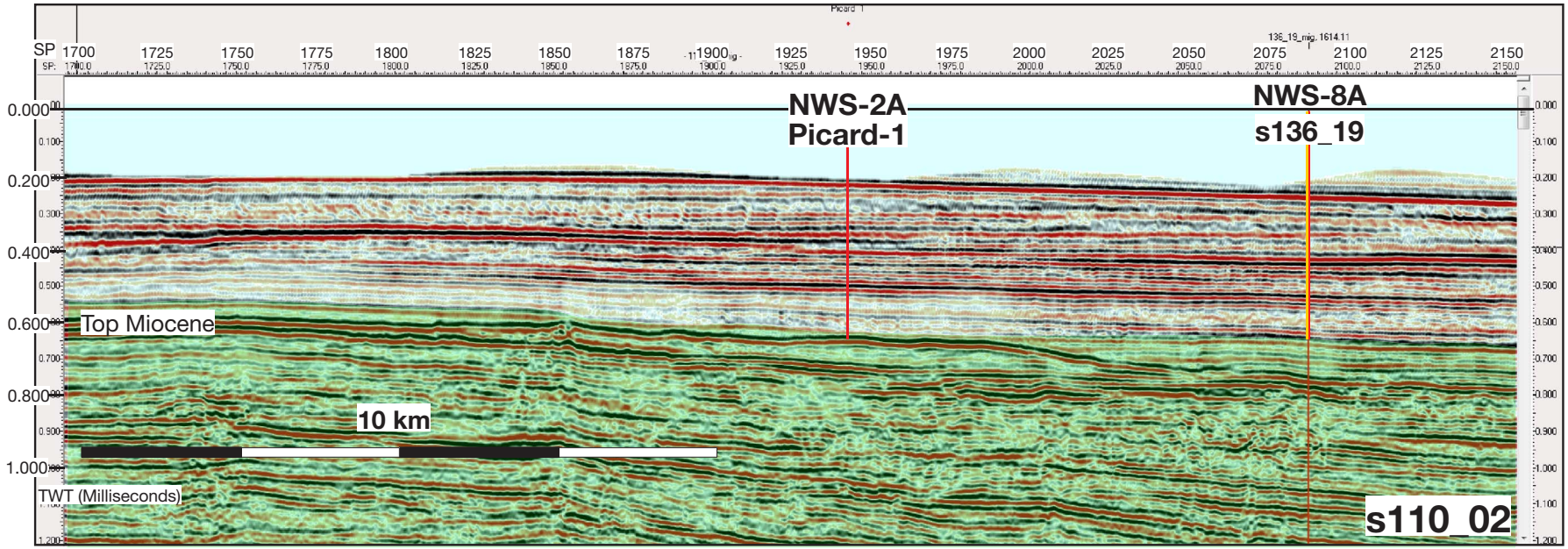

Figure AF13. Multichannel seismic profile across alternate Site NWS-8A. The top of the green shaded section is the inferred top of the Miocene. TWT = two-way traveltime.

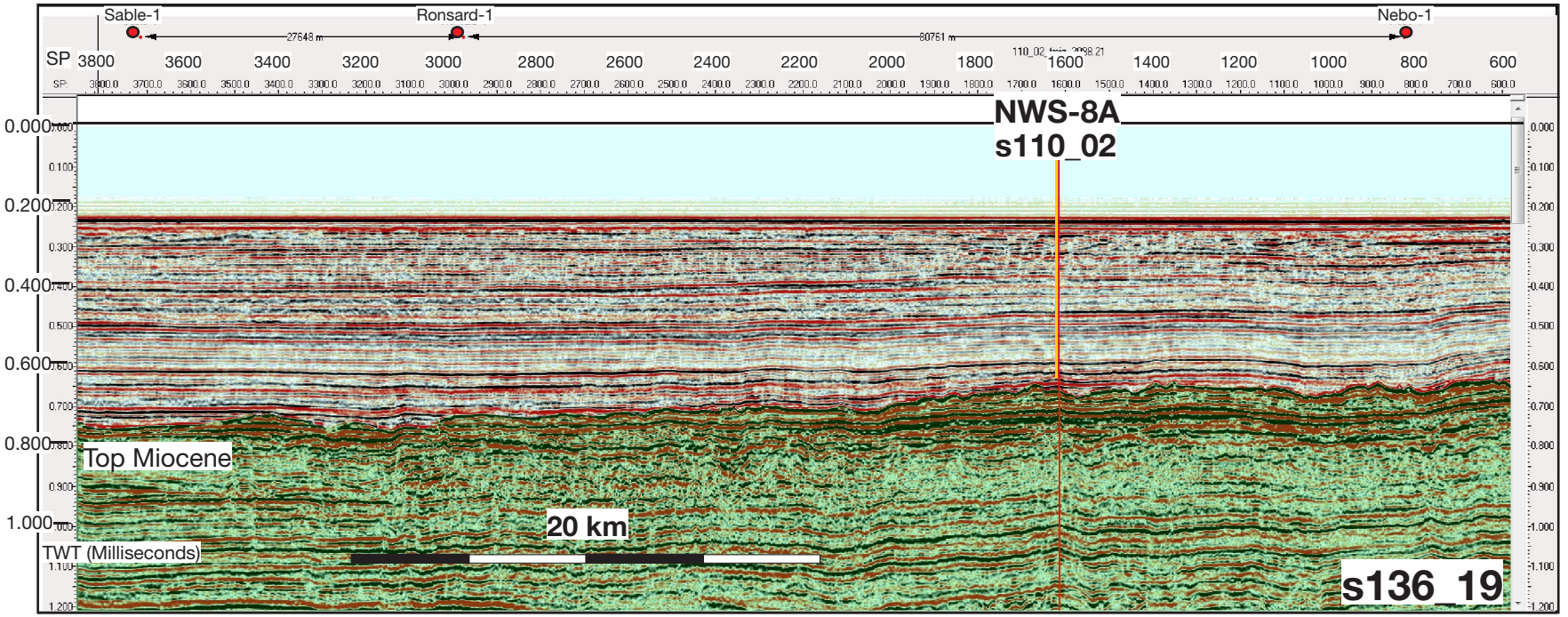

Figure AF14. Multichannel seismic profile across primary Site NWS-1A. The top of the green shaded section is the inferred top of the Miocene. TWT = two-way traveltime.

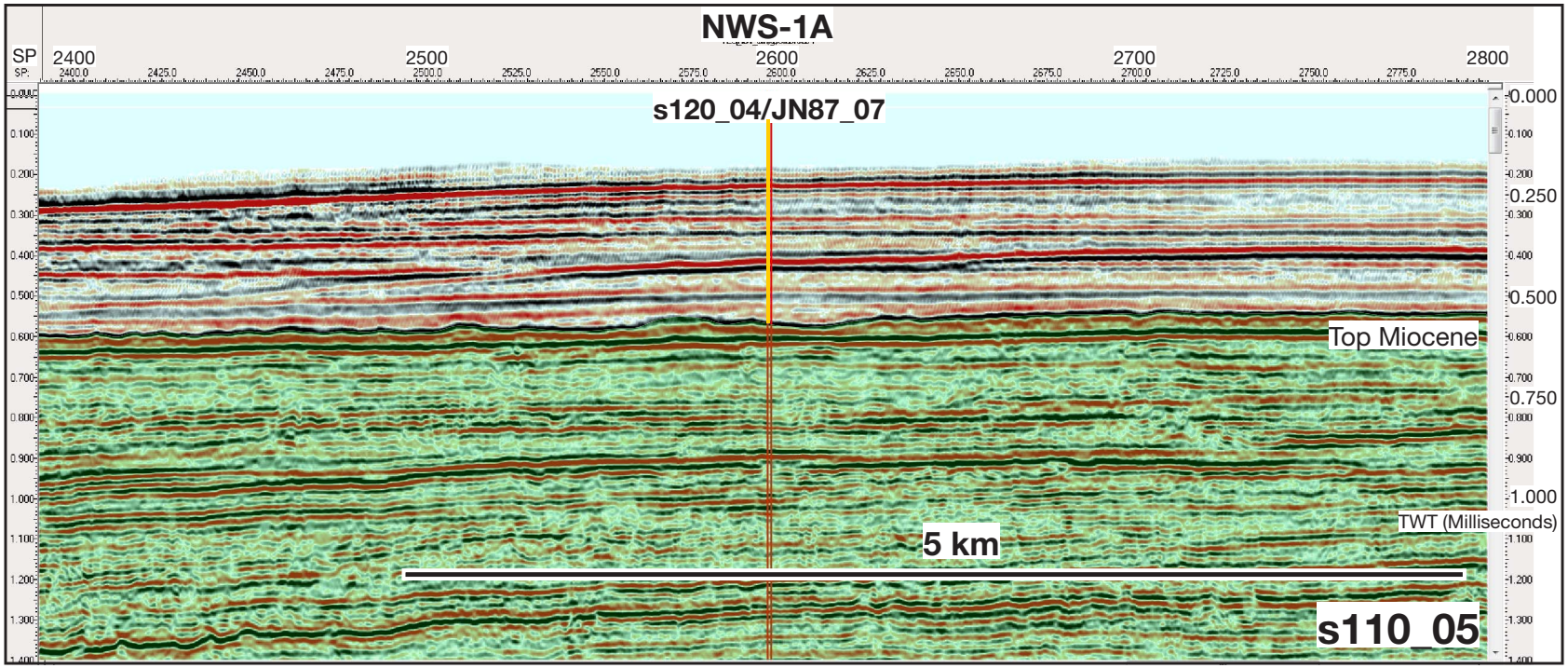

Figure AF15. Multichannel seismic profile across primary Site NWS-1A and alternate Site NWS-7A. The drowned shoal indicated is a fourth Rowley Shoal atoll that subsided from the sea surface to ~300 meters below sea level during the Pleistocene. Green line denotes the inferred top of the Miocene. TWT = two-way traveltime.

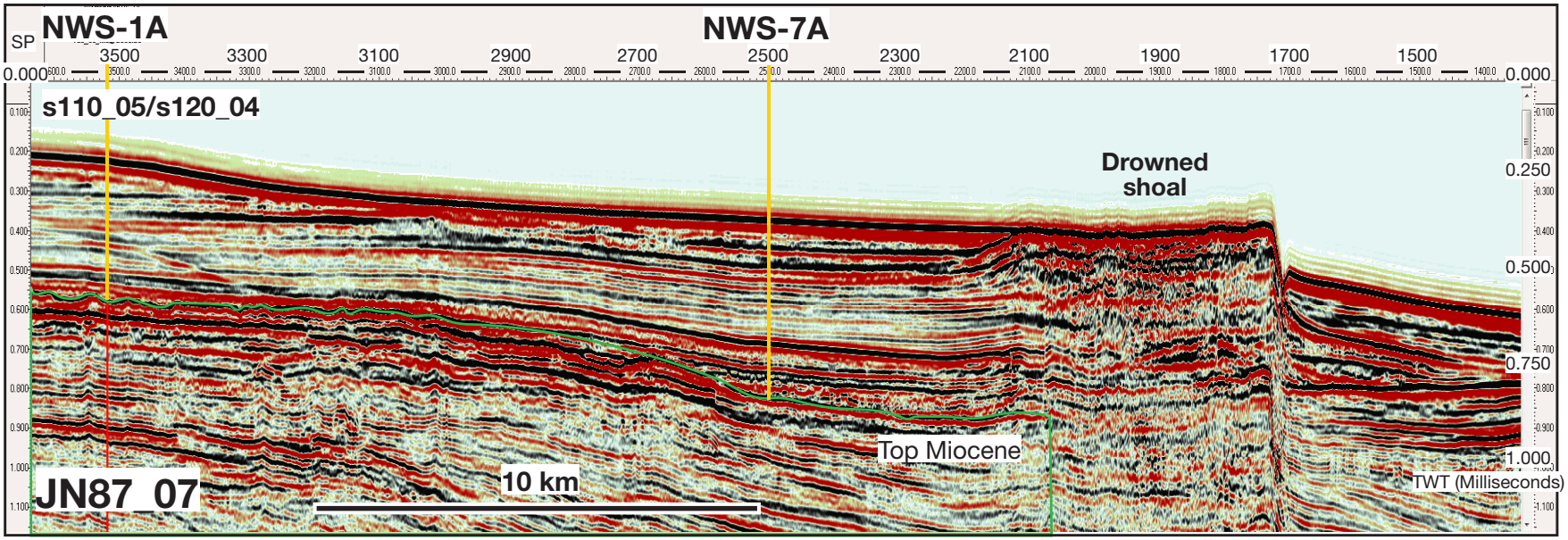

Expedition scientists and scientific participants

The current list of participants for Expedition 356 can be found at: **iodp.tamu.edu/scienceops/expeditions/indonesian_throughflow.html**